The Thesis Committee for Christopher Alexander Farley
Certifies that this is the approved version of the following Thesis:

Design, Synthesis, and Thermodynamic Evaluation of Peptidomimetic Ligands Binding to the Src SH2 Domain

APPROVED BY
SUPERVISING COMMITTEE:

Stephen F. Martin, Supervisor

Eric V. Anslyn

Design, Synthesis, and Thermodynamic Evaluation of Peptidomimetic Ligands Binding to the Src SH2 Domain

by

Christopher Alexander Farley

Thesis

Presented to the Faculty of the Graduate School of

The University of Texas at Austin

in Partial Fulfillment

of the Requirements

for the Degree of

Master of Arts

The University of Texas at Austin

May 2018

Dedication

To my wife Nicole, for her patience and support.

Acknowledgements

I must begin by thanking Prof. Stephen F. Martin for welcoming me into his group and for his guidance and wisdom. I have learned a great deal in the Martin group, and it begins with him. I also thank the members of Lab 2 who taught and guided me early in my time as a group member; in particular Caleb Hethcox, Alex Goodnough, and Lance Lepovitz. Lance and Zachary White were also a tremendous help with the biological aspect of my work. Special thanks must also be given to Michael Wood, Daniel Klosowski, and Zhipeng Wang for their friendship and support. I am particularly grateful to the NMR and mass spectrometry facilities and need to extend my thanks to Angela Spangenberg, Steve Sorey, Ian Riddington, and Vincent Lynch for their assistance in characterizing compounds.

I also thank my family for their support, love, understanding, and encouragement. My parents have always encouraged me to be the best I could be and I would not be in this position without them. Their enthusiasm and unrelenting positivity during adversity has been a tremendous blessing. My in-laws have been a great help as well, graciously opening their home in Houston for visits and providing time away from Austin to relax. Most importantly I need to thank my wife, Nicole, for her support through tough times and patience with the demands of graduate school.

Abstract

Design, Synthesis, and Thermodynamic Evaluation of Peptidomimetic Ligands Binding to the Src SH2 Domain

Christopher Alexander Farley, M.A.

The University of Texas at Austin, 2018

Supervisor: Stephen F. Martin

The ability to predict protein-ligand binding affinities is a difficult and elusive goal in the field of molecular recognition. Models exist to predict binding energetics; however, they are not always capable of considering the incidental events in ligand-binding due to the tendency of the Gibbs free energy ($\Delta G°$) to lack a correlation with enthalpy ($\Delta H°$), entropy ($\Delta S°$), or both. Binding studies of various pYEEI-derived peptidomimetic ligands to the Src SH2 domain were evaluated to investigate the effects of structural changes on protein-ligand binding energetics. The effect of preorganizing the pYEEI ligand into its binding conformation was analyzed by substituting the isoleucine residue with a conformationally constrained amino acid analog as well as a flexible analog. Isothermal titration calorimetry studies were performed to assess the effects of ligand structure on protein-ligand binding energetics.

Table of Contents

List of Tables

List of Figures

List of Schemes

Chapter 1: Thermodynamics of Protein-Ligand Interactions

1.1 INTRODUCTION

Among the major challenges in rational drug design and understanding molecular recognition processes in biological systems is how changes in the structure of small molecules affect their affinities for a protein target. When a drug lead is discovered, efforts to improve the binding affinity to its target are undertaken by altering the molecular structure. Critical to this endeavor is the ability to anticipate the binding energetics in protein-ligand interactions. Predicting these interactions is complex, because one must consider a multitude of events that occur during binding, including protein dynamics, solvent, ligand, and protein reorganization.

Models exist to predict binding energetics; however, they are not always capable of considering the incidental events in ligand-binding due to the tendency of Gibbs free energy ($\Delta G°$) to lack a correlation with either enthalpy ($\Delta H°$), entropy ($\Delta S°$), or both.[1-4] There is a vast amount of data on protein-ligand binding; however, most of it is limited to binding affinity (K_a) with no corresponding information of the entropies and enthalpies of the binding event.[3] Due to the lack of studies that investigate enthalpy and entropy of binding, there remains an uncertainty of how changes in $\Delta H°$ and $\Delta S°$ correlate with changes to ligand structure. The inadequate tools available for predicting these energies have provided the impetus to evaluate the thermodynamic effects of introducing incremental structural changes to related ligands in protein binding interactions.

Numerous strategies to optimize binding affinity are employed to increase $\Delta H°$ and $\Delta S°$. Increasing $\Delta H°$ most commonly includes alterations designed to increase noncovalent interactions.[1,5-7] Strategies to optimize these stabilizing forces tend to lead to significant challenges due to the unfavorability of desolvating a polar group. Furthermore, polar contacts in protein-ligand interactions, such as hydrogen bonding, tend to be highly dependent upon distance and angle, and even subtle perturbations that alter the orientation of polar groups can have dramatic effects on protein-ligand binding.[8] Enhancing van der Waals contacts is conceivably easier in the sense that the strength of nonpolar contacts is determined by the distance between the nonpolar groups and the geometry of the contacts is not important. Enhancing nonpolar contacts is not often used as a strategy to improve $\Delta H°$ of binding, but rather $\Delta S°$ and will be discussed in the next section.

1.2 Structural Effects on Binding Energetics

One strategy to enhance $\Delta S°$ of binding is to preorganize the ligand into its biologically active conformation, which conventional wisdom dictates should reduce ligand entropy.[5] Since ligands in solution do not predominantly exist in their bound conformation, they must reorganize to adopt the conformation in which they bind to their biological target.[10] This reorganization is generally unfavorable because there is a decrease in entropy upon adopting a well-defined conformation.[10-12] Global and local constraints have been utilized as methods to lock the molecule into its bound conformation. The restriction of bond rotation, or the number of rotors, in the ligand reduces the entropy of the molecule in solution.[13] However, minimizing the entropy term by preorganizing the

ligand in its biologically active conformation has not always translated into the predicted favorable changes in Gibbs free energy for ligand complexation with the protein.[14-16]

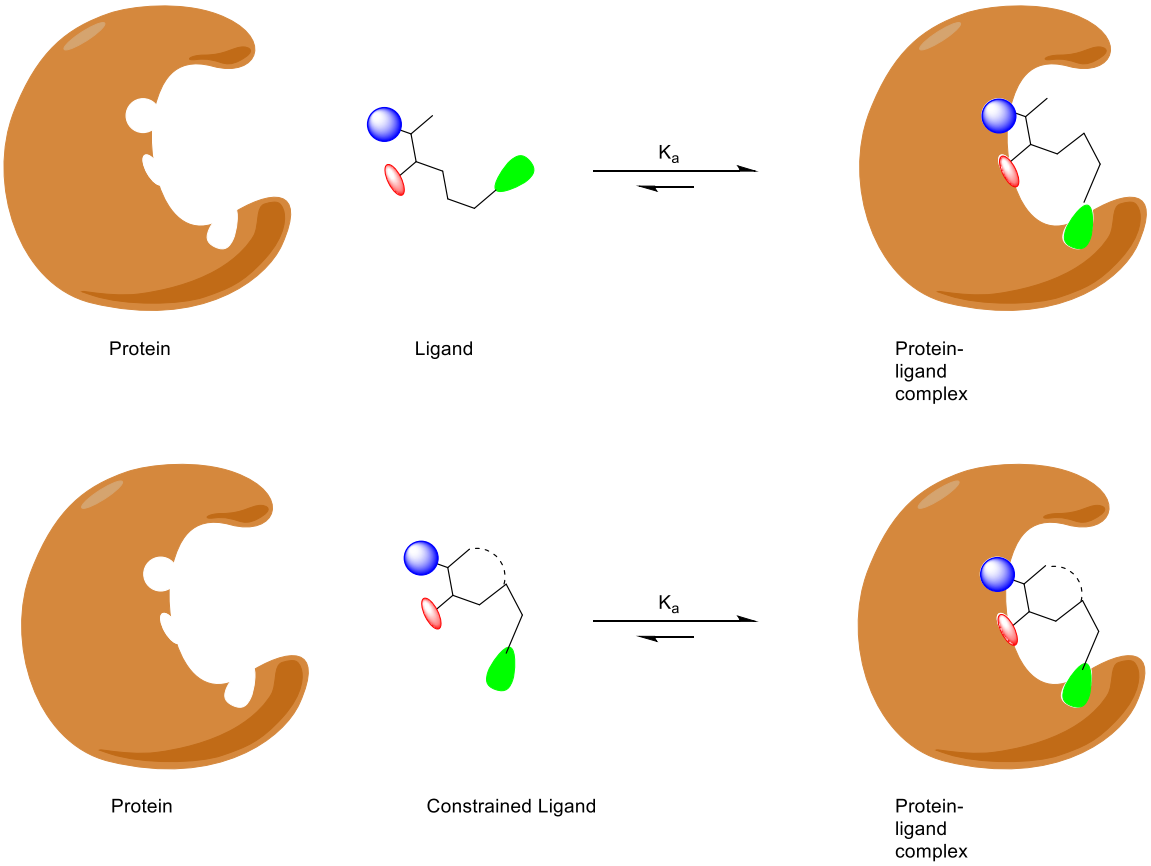

Figure 1: Graphical representation of protein-ligand binding event.
The top ligand is free to rotate while in solution, whereas that mobility is restricted in the constrained ligand.

Another approach to enhancing binding affinity by improving ΔS° that has been used exploits the hydrophobic effect. The hydrophobic effect is associated with the

tendency of nonpolar groups to aggregate in an aqueous environment, which in the context of protein-ligand interactions means that hydrophobic areas of a ligand will tend to be buried into hydrophobic regions of the protein upon binding.[17,18] The solvation of polar and nonpolar groups by water leads to a loss of entropy, as the water molecules form an ordered network of hydrogen bonds to encapsulate the solute. Upon ligand binding, the water molecules that solvate both the ligand as well as the protein are released to the bulk, which leads to an increase in degrees of freedom of water and thus a more favorable $\Delta S°$.[17] However, since the proteins and ligands tend to be dynamic, the entropic component of this process is not the only thermodynamic parameter that can be considered in predicting binding affinities.[18-19] Instead, if the structures of the ligand or protein are such that a hydrogen bonding network cannot be established in solution, the binding event can be enthalpically driven.[20] The complex nature of the effects of hydrophobic interactions on protein-ligand binding, in particular on the discrete $\Delta H°$ and $\Delta S°$ components, remains an under-investigated topic of experimentation.

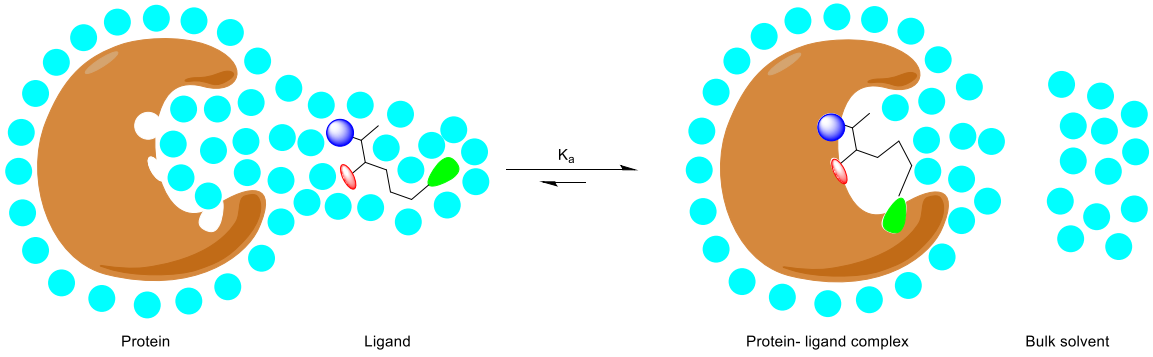

Figure 2: Depiction of water solvation in protein-ligand interactions.

As previously noted, attempting to increase binding affinities of ligands to their targets is a challenge due to the unpredictability in how modifications to ligand structures will affect the binding enthalpies and entropies. It has often been found that in efforts to optimize either $\Delta H°$ or $\Delta S°$ there is a compensatory effect in the other parameter such that the overall $\Delta G°$ of binding does not changes significantly.[21] Enthalpy-entropy compensation is almost universally observed in protein-ligand interactions,[22,23] prompting studies to determine whether this effect is an obligatory feature in such interactions.[24] Regardless of whether the enthalpy-entropy compensation is an inherent property of molecular recognition, the fact remains that preorganization is a proven strategy for enhancing affinity although the reasons why are not always well understood, and the benefits may be marginal or nonexistent.[25]

1.3 ISOTHERMAL TITRATION CALORIMETRY

Isothermal titration calorimetry (ITC) is a technique that allows one to determine thermodynamic parameters in a single experiment, including binding stoichiometry (n), K_a, $\Delta H°$, $\Delta S°$, and $\Delta G°$.[27,28] ITC is commonly used for its simple operation, accuracy, and ability to determine the aforementioned variables in a single experiment. Traditionally, only K_a and $\Delta G°$ were easily determined, whereas elucidating $\Delta H°$ and $\Delta S°$ required multiple binding experiments at different temperatures in order to reliably calculate the values via a van't Hoff analysis,[27] using the equation:

$$lnK_a = -\frac{\Delta H°}{RT} + \frac{\Delta S°}{R}$$

where T is the temperature (Kelvin) and R is the ideal gas constant (1.985 cal/mol•K). Plotting $\ln(K_a)$ against T^{-1} gives a straight line where the slope is $\Delta H°/R$, and the y-intercept is $\Delta S°/R$. The analysis requires many experiments at variable temperatures in order to acquire results with good reliability. Because K_a is temperature-dependent, even slight deviations in slope leads to errors in both entropy and enthalpy. Due to the requirement of many repeated error-prone experiments, van't Hoff analyses have fallen out of favor as a means to determine $\Delta S°$ and $\Delta H°$ with the rise in popularity of ITC.

In an ITC experiment, solutions containing the ligand are injected to a sample cell containing a solution of protein. After an injection, the instrument measures the power necessary to maintain the same temperature as a reference cell. The measured power is plotted as a function of time, and then the area under the curve is integrated and plotted against the molar ratio between the ligand and protein. From this second curve, $\Delta H°$ is determined by integrating the power required to maintain the same temperature throughout the experiment. Binding affinity is the slope of the line tangent to the inflection point of the curve. Given K_a and $\Delta H°$, $\Delta G°$ and $\Delta S°$ can be calculated by the equations:

$$\Delta G° = -nRT\ln(K_a)$$

$$\Delta G° = \Delta H° - T\Delta S°$$

where temperature (T, Kelvin) is set in the experiment. The rapid and operationally simple ITC experiments are an invaluable tool for examining energetics of binding events. Changes in binding affinity from one ligand to another to the same protein can be readily investigated by examining $\Delta S°$ and $\Delta H°$ of the binding event.

1.4 SRC SH2 DOMAIN

The Martin group became interested in exploring the complexities of how ligand preorganization impacts protein-ligand interactions in the 1990s and initiated a research program to investigate the mysteries of the field. Small ligands derived from peptides, or peptidomimetics, were selected as the chemical probes for the binding events because of their use as therapeutics in modern pharmaceuticals and due to the relative ease of modulating each amino acid residue on the ligand.[29-30] The ability to incrementally alter the ligand structures is key to understanding the source of any changes in binding that may occur. The initial thrust into this field of inquiry tested the binding of the Src SH2 domain (sarcoma homology 2 domain of the sarcoma tyrosine kinase protein) and a truncated version of its endogenous ligand.

The first protein of interest for this new research program was Src, a tyrosine kinase involved in signaling pathways that cause bone resorption and it was identified as a potential target for the treatment of osteoporosis, sarcomas, and other diseases of the bone.[31] As a result of the interest Src received from both academia and industry, there was a wealth of information available about the protein. Among the most important things that were known about Src was that the SH2 domain bound with a 1:1 stoichiometry with its endogenous ligand, it had a well-defined binding site, and the protein does not undergo a significant structural change upon ligand binding.[31,32] Seminal thermodynamic investigations were performed by Waksman and coworkers, who performed site mutagenesis studies on both the Src SH2 protein and the peptide ligand PQpYEEIPI. Their investigations revealed that the pYEEI region of the ligand is the most important portion

for the binding event and engages in a so called "two-pronged plug two-holed socket" binding mode wherein the pY residue occupies a polar pocket and the Ile residue resides in a nonpolar pocket.[33,34] Subsequent investigations by the Waksman group found that the pY residue is critical for binding in one pocket and found that the removal of a nonpolar side chain at the +3 site led to a much lower affinity binding event (pYEEI K_a = 5.5 x 10^6, pYEEG K_a = 2.6 x 10^5).[35,36] They also replaced other residues of the ligand and found that replacing the two glutamate residues also led to a loss in binding affinity, but markedly less so than the replacement of pY or Ile.

1.5 Previous Martin Group Work

1.51 Src SH2

The Martin group was inspired by these reports and embarked on a study of 1,2,3-trisubstituted cyclopropyl ligand derivatives of the native ligand for the Src SH2 with the intent of probing the effects of preorganizing the pY site in its binding conformation. Analysis of the Src SH2-ligand co-crystal structure indicated that the phosphotyrosine residue adopted a gauche conformation with respect to the ligand backbone, which could be approximated through the introduction of a cyclopropane ring.[37] The so called "native" tetrapeptide pYEEI, constrained peptide mimic (cpYEEI), and flexible analog (fpYEEI) were synthesized and evaluated for binding in ITC studies. The tetrapeptide subunit is the region of the endogenous ligand, the 11-mer peptide EPQpYEEIPIYL, that is in direct contact with the protein in the binding event. The "reverse amide" moiety found in compound **2** was installed in order to maintain the same number of heavy atoms (in this

context, heavy atoms refer to any atom other than hydrogen) in order to accommodate the cyclopropane ring. The reverse amide also maintains the relative position of the carbonyl group in the ligand so that changes to the structure were minimized. Ligand **3** was prepared to serve as a flexible analog of **2** to account for altering ligand **1** to include the reversed amide functionality.

As seen in Table 1, the constrained ligand **2** had a more favorable $\Delta S°$ of binding compared to its flexible counterpart **3** and the native ligand **1**, as hypothesized. This was an exciting result because this was the first experiment that supported the long-standing adage that preorganization of ligands enhances entropy of binding. Despite the enhanced $\Delta S°$, the constrained ligand suffered an enthalpic penalty. The enthalpy-entropy compensation that occurred led to a negligible difference in $\Delta G°$ between each of the ligands, although there was a slight benefit for **2** over its flexible counterpart, **3**, and both over the native ligand.

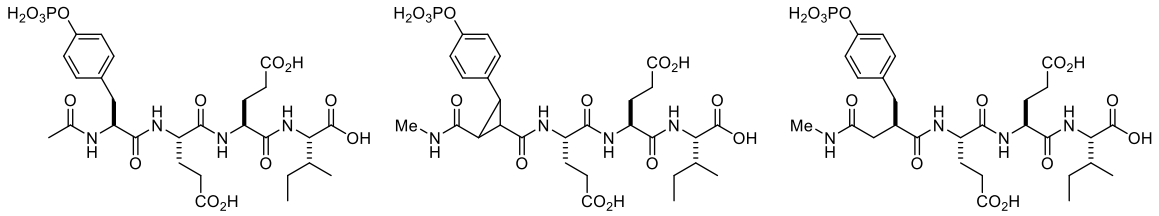

1 2 3

Ligand	K_a (M^{-1})	$\Delta G°$ (kcal mol^{-1})	$\Delta H°$ (kcal mol^{-1})	$-T\Delta S°$ (kcal mol^{-1})
1	4.1 (± 0.1) 10^6	-9.01 ± 0.01	-6.06 ± 0.05	-2.95 ± 0.07
2	1.0 (± 0.1) 10^7	-9.55 ± 0.07	-5.91 ± 0.04	-3.64 ± 0.13
3	1.7 (± 0.1) 10^7	-9.80 ± 0.20	-7.33 ± 0.03	-2.47 ± 0.20

Table 1: Binding data of ligands **1-3** binding to Src SH2 domain.[37]

In an attempt to discover the source of the enthalpic compensation that was observed in this experiment, the Martin group turned to X-ray crystallographic studies to compare the structures of each of the modified ligands bound to the protein to the bound native ligand (Src SH2-**1**). The crystal structure of the Src SH2 complex was compared to the Src-bound 11-mer peptide EPQpYEEIPIYL, which as previously mentioned is the endogenous ligand that binds to the Src SH2 domain. Few structural differences were discovered in comparing the crystal structures of the truncated tetrapeptide to the longer peptide in the binding region, which validated the choice to use the synthetically simpler tetrameric peptide instead of the 11-mer in the studies that were to follow.[33] Comparing the X-ray crystal structures of bound ligand **1** to bound ligand **2** revealed only minor differences in the binding conformations at the pY site and the pY+3 site (Figure 3A); these

two sites, as previously mentioned, are the sources of nearly all the binding energy. There do exist differences in conformation at the pY+1 and pY+2 sites, however, while the differences were spatially significant they were determined not to be energetically consequential. The variance in positions of both glutamate residues within asymmetric units of the crystal structures of a protein-ligand complex indicated that variations between different protein-ligand complexes were within the margins of error.[36,37] Meaningful structural differences emerged upon comparing the flexible ligand, **3**, to ligands **1** and **2**, most notably at the pY site (Figure 3B, 3C). The pY residue of **3** had a different orientation of both the methyl amide as well as the phenol phosphate group of the amino acid. The amide nitrogen of **3** was able to engage in an intramolecular water-bridged hydrogen bond with the phosphate group, an interaction not observed in **1** (Figure 3B) and geometrically unattainable in ligand **2** due to the restrictive cyclopropane (Figure 3C). This new interaction coincided with a loss of the hydrogen bond between the oxygen atom of the carbonyl group of the amide and the protein, though it also gained a water-mediated contact with the protein.

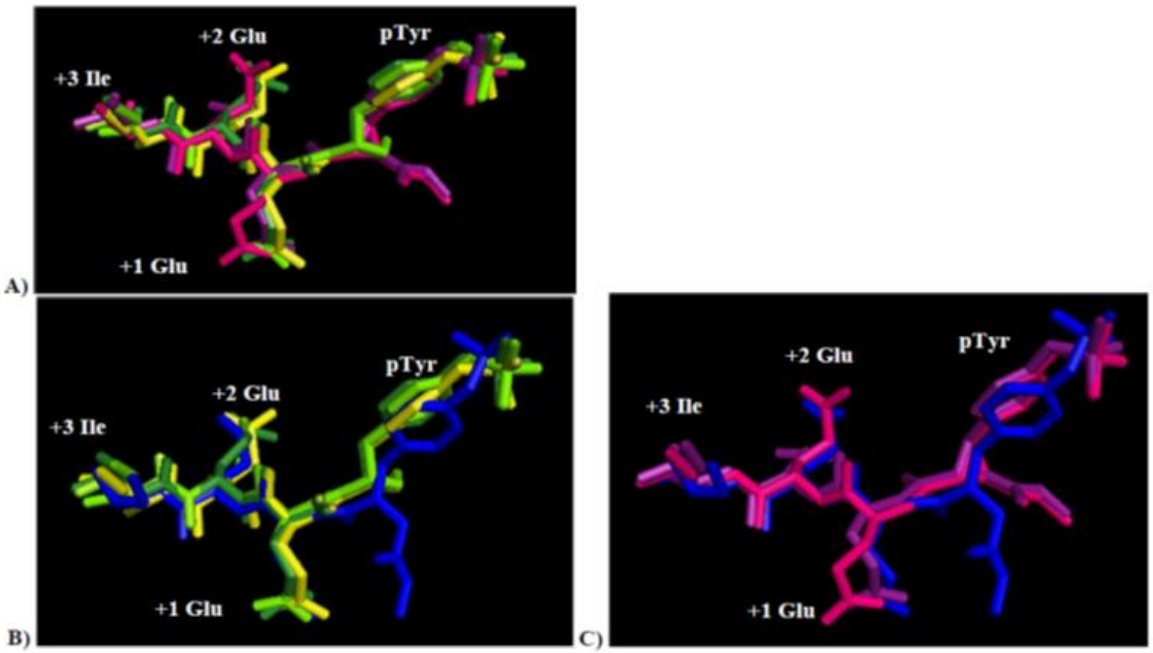

Figure 3: X-ray crystal structures of ligands **1**-**3** bound to Src SH2 domain.

A) Overlay of both poses of pYEEI complexes in the asymmetric unit (yellow and green) with both poses of constrained ligand **2** complexes in the asymmetric unit (pink and purple). **B)** Overlay of both poses of pYEEI complexes in the asymmetric unit (yellow and green) with flexible ligand **3** complexes in the asymmetric unit (blue). **C)** Overlay of both poses of ligand **2** complexes in the asymmetric unit with ligand **3** complexes in the asymmetric unit.[38]

Although X-ray crystallography is an invaluable tool for examining protein-ligand interactions, it is not without limitations. Protein-ligand interactions occur in solution; therefore, a solid state structural analysis will invariably lack information about the dynamic process. That subtle differences between the crystal structures of **1** and **2** could correspond to significantly different binding thermodynamics were puzzling and warranted

further investigation. Accordingly, Martin and Post examined the protein structures using nuclear magnetic resonance (NMR) and molecular dynamics (MD) studies.[39] In the ^{1}H-^{15}N HSQC experiments, the Src SH2-ligand complexes were examined for chemical shift perturbations (CSPs) and chemical shift differences (CSDs). CSPs are the changes observed in Src SH2 amide N-H resonances upon complexation of the ligand to the protein, and CSDs are the differences in CSP magnitudes between each protein-ligand complex and the *apo*-protein (*ie*, protein with no bound ligand). These experiments showed that significant CSPs occurred at the residues in the phosphotyrosine binding site. The CSPs showed that there was an increase of deshielding effects, indicating altered hydrogen bonding interactions.[39,40]

Figure 4 illustrates a stark difference in the chemical environments of the E178 and R175 residues in the Src SH2 binding site in the different protein-ligand complexes. The binding of flexible ligand **3** to the protein led to the greatest chemical shift of the E178 and R175 protons as compared to the *apo* protein, followed by the native ligand **1**, and constrained ligand **2**. These CSDs correlated with the observed trends of $\Delta H°$ from ITC experiments: The Src SH2-**3** complex had the strongest CSD as well as the most favorable $\Delta H°$, followed by the Src SH2-**1**, and then the Src SH2-**2** complexes, the last of which had the smallest CSD and the least favorable $\Delta H°$. This trend indicates that the hydrogen bonding interactions are strongest in the flexible ligand, and weakest in the constrained ligand, consistent with the enthalpic cost that was observed in the ITC experiments.[19]

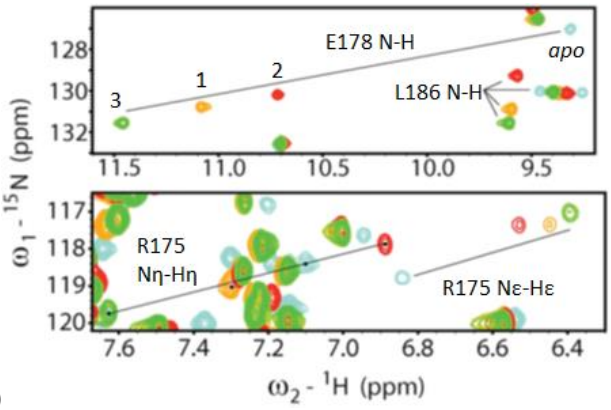

A)

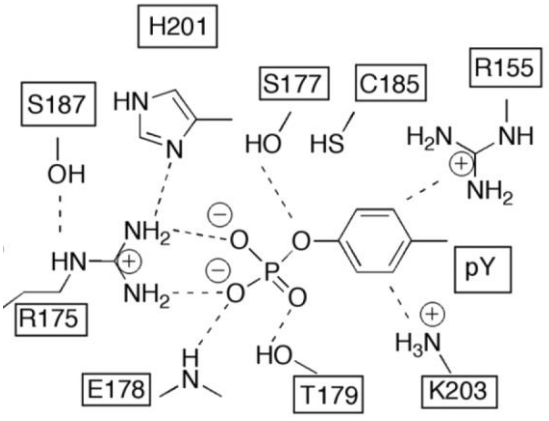

B)

Figure 4: NMR studies of ligands **1**-**3** binding to Src SH2 domain.

A) ^{1}H-^{15}N HSQC of *apo*-Src SH2 (cyan), ligand **1**-Src SH2 adduct (yellow), ligand **2**-Src SH2 adduct (red), ligand **3**-Src SH2 adduct. **B)** Diagram of protein-ligand binding interactions at the pY-site of Src SH2.[39]

1.52 Grb2 SH2 Domain

ITC experiments analogous to those performed on Src SH2 were carried out on another model protein, the SH2 domain of the growth receptor binding protein 2, or Grb2 SH2.[41] The Grb2 SH2 domain is an adapter protein responsible for cell proliferation and differentiation via the Ras pathway, stimulating interest in Grb2 SH2 as an anticancer drug target.[41,42] Ligands **4**-**15** were prepared as truncated versions of the endogenous ligand and evaluated in the same manner as the ITC studies on ligands **1**-**3**. There was an enhancement of K_a and $\Delta G°$ in the constrained ligands, but this was accompanied by an unexpected less favorable $\Delta S°$. The enhanced $\Delta G°$ was a result of the more negative $\Delta H°$ values overpowering the relatively unfavorable entropic component in the constrained molecules.

To elucidate the source of the confounding thermodynamic parameters, X-ray crystal structures of the protein-ligand complexes were analyzed. Though both the flexible and constrained analogs bound in nearly identical conformations, the constrained ligands appeared to be involved in more direct polar contacts, which correlated with a more favorable $\Delta H°$ of binding. Complicating the matter, however, was that the flexible ligands bound to the protein with more water-mediated contacts such that the number of total contacts was about the same as the constrained ligands. These studies indicate that despite thermodynamic analyses and X-ray crystal structures to characterize binding events, there is a significant lack of understanding of protein-ligand interactions, especially the involvement of water in establishing polar contacts between the ligand and protein.

To shed light on the unexpected thermodynamic consequence between constraining the pY component of the ligand and its binding to the two different proteins, computational

studies were performed by collaboration with the Ren group on three sets of constrained and flexible analogs: Ligands **4** and **5**, ligands **6** and **7**, and ligands **10** and **11**.[43] One major finding from these molecular dynamics simulations was that a significant portion of the solution-state flexible ligand appeared to be stabilized by an intramolecular hydrogen bond between the phosphate group and the two amide groups of asparagine. The constrained ligands were not able to adopt a conformation that permitted intramolecular hydrogen bonding, and thus were calculated to have higher solution state entropy as compared to the flexible ligand. It may appear counterintuitive for the flexible ligand to be more preorganized, because the solution state conformation differs from the binding conformation to a large degree. Bear in mind that since entropy is a state function (*ie,* the path by which a system converts from one state to another does not matter), the relatively highly-ordered solution state of the flexible ligands as compared to the constrained ligands therefore leads to a lesser differential of entropy between the solution and the ordered bound states, even though the bound conformation of the flexible ligand completely differed from the preferred solution-state conformation.

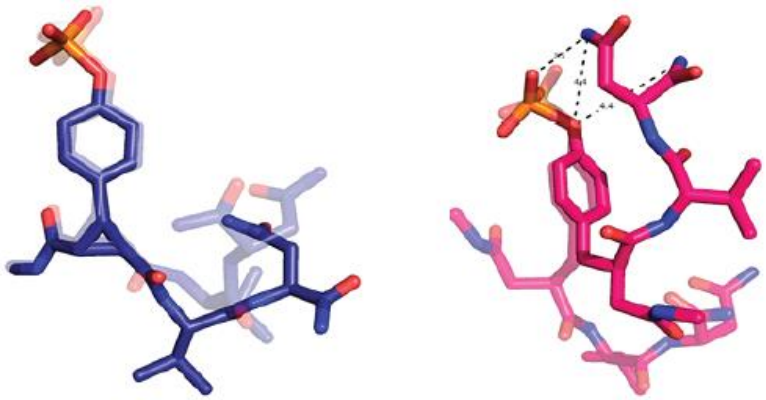

Figure 5: MD-predicted solution state structures for ligands **4** and **5**.
Left: MD simulation of ligand **4** in solution, transparent conformation from crystal structure; Right: MD simulation of **5** in solution with macromolecular hydrogen bonds shown, transparent conformation from crystal structure.

The ITC studies on modifying the ligands at the pY unit resulted in different thermodynamic profiles between the Src SH2 and Grb2 SH2 domains. This is not completely unexpected given that the major stabilizing forces at the pY-binding site are hydrogen bonds, which are highly dependent on both distance and angle between the donor and acceptor. A modification to this residue could have amplified and unpredictable thermodynamic consequences, and these examples provided two opposite results wherein the constrained pYEEI ligand bound with a more favorable $\Delta S°$ of binding to Src SH2 but the constrained pYVN ligand bound with a more favorable $\Delta H°$ of binding to Grb2 SH2.

In addition to evaluating the effects of ligand preorganization, the Martin group has also examined the effects of increasing hydrophobic surface area upon energetics in protein-ligand interactions. As noted earlier, increasing hydrophobic surface area is a tactic

that is normally used to enhance K_a by making binding more entropically favorable. [44] Ligands **16**-**23** were prepared with a straight-chain alkyl series **16**-**19** of pseudopeptides as well as a cyclic alkyl series **20**-**23**.

In general, for the ligands **16**-**19** there was little difference between the K_a and $\Delta G°$ values as chain length increased from ethyl to *n*-pentyl. There does appear to be a slight benefit to enthalpy with a concomitant less favorable entropy for ligands **18** and **19**, the ligands with n-butyl and *n*-pentyl as the R groups for the pY+1 amino acids; however, those values fall at the outer bounds of the margin of error. It was determined by X-ray crystal structure analysis that ligands **18** and **19** make more van der Waals contacts with the protein than ligands **16** and **17**, leading to a more favorable $\Delta H°$ of binding. The less favorable $\Delta S°$ of binding may arise from the number of rotatable bonds being greater for ligands **18** and **19** than in the ligands with shorter R group chain lengths. Recall that preorganization of ligands by restricting rotors is hypothesized to lead to a more favorable entropy of binding.

There exists a clear trend of increasingly favorable K_a's and $\Delta G°$s as cycloalkane size increases from cyclopropyl to cyclohexyl for ligands **20**-**22**. Interestingly, this trend was driven by a more favorable $\Delta H°$ of binding and not $\Delta S°$ of binding. As mentioned in section 1.2, the general hypothesis is that increasing nonpolar surface area leads to a more favorable $\Delta S°$ of binding due to the release of water molecules solvating the protein and ligand to the bulk. The studies indicated that there was no correlation of the heat of solvation for the ligands with the increase in hydrophobic surface area, nor was there a correlation between the number of water molecules at the protein-ligand interface and the

entropy of binding. This study again highlights the difficulties in understanding the role of structure on the energetics of protein-ligand interactions and the need for more studies on this phenomenon in order to better predict the effects of structural changes on protein-ligand binding.

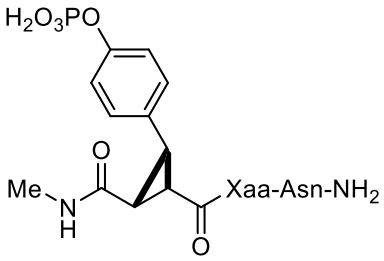

4: Xaa = Val
6: Xaa = Ile
8: Xaa = Leu
10: Xaa = Gln
12: Xaa = Glu
14: Xaa = Lys

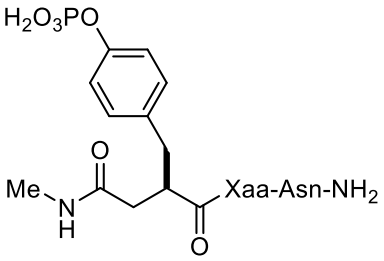

5: Xaa = Val
7: Xaa = Ile
9: Xaa = Leu
11: Xaa = Gln
13: Xaa = Glu
15: Xaa = Lys

Ligand	K_a (M^{-1})	$\Delta G°$ (kcal mol^{-1})	$\Delta H°$ (kcal mol^{-1})	$\Delta S°$ (cal mol^{-1})
4	2.8 (± 0.02) 10^6	-8.8 ± 0.02	-7.9 ± 0.29	3.0 ± 0.30
5	4.5 (± 0.12) 10^5	-7.7 ± 0.02	-5.4 ± 0.14	7.9 ± 0.22
6	2.1 (± 0.08) 10^6	-8.6 ± 0.02	-8.3 ± 0.30	1.3 ± 0.30
7	4.1 (± 0.15) 10^5	-7.7 ± 0.02	-5.5 ± 0.20	7.4 ± 0.30
8	7.1 (± 0.27) 10^5	-8.0 ± 0.02	-6.0 ± 0.22	6.6 ± 0.30
9	1.7 (± 0.06) 10^5	-7.1 ± 0.02	-4.6 ± 0.17	8.6 ± 0.30
10	1.2 (± 0.06) 10^6	-8.3 ± 0.01	-9.8 ± 0.20	-5.2 ± 0.18
11	5.6 (± 0.15) 10^5	-7.8 ± 0.02	-8.7 ± 0.23	-2.8 ± 0.22
12	3.6 (± 0.10) 10^5	-7.6 ± 0.02	-10.3 ± 0.27	-9.0 ± 0.22
13	3.0 (± 0.08) 10^5	-7.5 ± 0.02	-8.8 ± 0.23	-4.3 ± 0.22
14	5.5 (± 0.15) 10^5	-7.8 ± 0.02	-9.2 ± 0.24	-4.6 ± 0.22
15	9.8 (± 0.23) 10^4	-6.8 ± 0.02	-7.7 ± 0.20	-3.0 ± 0.21

Table 2: Binding data for ligands **4-15** binding to Grb2 SH2 domain.[41]

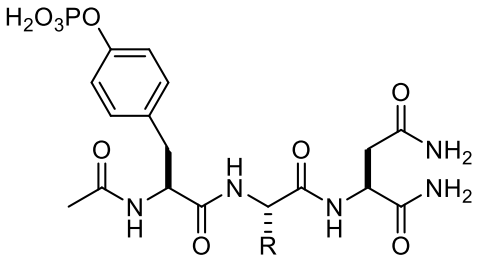

16: R = ethyl
17: R = *n*-propyl
18: R = *n*-butyl
19: R = *n*-pentyl

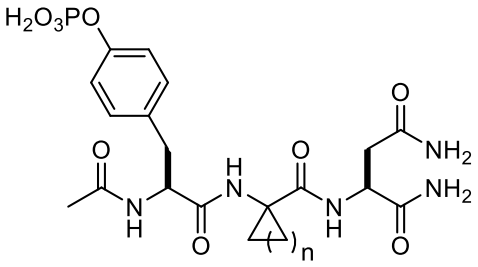

20: n = 1
21: n = 2
22: n = 3
23: n = 4

Ligand	K_a (M^{-1})	$\Delta G°$ (kcal mol^{-1})	$\Delta H°$ (kcal mol^{-1})	$-T\Delta S°$ (kcal mol^{-1})
16	8.6 (± 0.20) 10^5	-8.1 ± 0.1	-6.8 ± 0.5	-1.3 ± 0.1
17	7.6 (± 1.0) 10^5	-8.0 ± 0.1	-6.7 ± 0.5	-1.3 ± 0.3
18	8.4 (± 0.60) 10^5	-8.1 ± 0.1	-7.3 ± 0.3	-0.8 ± 0.2
19	7.8 (± 0.60) 10^5	-8.0 ± 0.1	-7.2 ± 0.3	-0.8 ± 0.2
20	1.6 (± 0.1) 10^5	-7.1 ± 0.1	-3.3 ± 0.3	-3.8 ± 0.1
21	4.3 (± 0.4) 10^5	-7.7 ± 0.1	-5.4 ± 0.3	-2.3 ± 0.2
22	16.1 (± 1.1) 10^5	-8.5 ± 0.1	-6.3 ± 0.4	-2.2 ± 0.2
23	69.6 (± 12.) 10^5	-9.3 ± 0.1	-8.5 ± 0.4	-0.8 ± 0.4

Table 3: Binding data for ligands **16-23** binding to Grb2 SH2 domain.[44]

1.6 SUMMARY AND CONCLUSIONS

The Martin group has examined several different systems toward gaining a better understanding of the thermodynamics of binding and the implications of installing conformational constraints into small molecules. Conventional wisdom would suggest that ligand preorganization should enhance binding affinity by reducing the entropic penalty upon binding. The notion that enhancements in binding affinities of preorganized ligands

is primarily due to a more favorable entropy of binding has been tested by performing ITC experiments on how ligands bind to proteins, incrementally and systematically altering each ligand in order to examine the different thermodynamic profiles of each binding event.

ITC experiments performed on the Src SH2 domain revealed that the hypothesis that preorganization of ligands leads to an enhancement of binding entropy holds for this system.[37] Unexpectedly, however, the flexible counterparts to the constrained ligands were nearly equipotent in binding ($\Delta G°$ and K_a), because there was a lower $\Delta H°$ of binding for the constrained ligand compared to the flexible ligand. The phenomenon of entropy-enthalpy compensation remains an interesting, if at times frustrating, facet of the energetics of protein-ligand interactions. In this example, introducing a conformational constraint at a residue that was involved in hydrogen bonding interactions with the protein was found to have a detrimental effect on $\Delta H°$ of binding to compensate for the enhancement to $\Delta S°$ of binding. The flexible analog was able to engage in stronger hydrogen bonding interactions between the phosphotyrosyl side chain of the ligand and the protein, which led to a more favorable $\Delta H°$ of binding.

Analogous binding studies performed on the Grb2 SH2 domain returned the confounding result that conformationally constrained ligands actually bound with a less favorable $\Delta S°$ of binding compared to their flexible controls.[41] These results were maybe a result of the flexible analog having a lower solution state entropy than the constrained ligand, which MD studies suggest is due to the presence of stabilizing macrocyclic hydrogen bonding interactions within the ligand.[43] The ligand that was preorganized into its binding conformation therefore was actually less “preorganized” than the ligand

intended to have more degrees of freedom. This finding was astonishing in that there was evidence that constraining a small molecule into its binding conformation could actually be less preorganized than a structurally similar molecule that adopted a solution state conformation that did not resemble the binding conformation at all.

Other studies on the Grb2 SH2 system revealed that increasing hydrophobic surface area enhanced binding affinity due to more favorable enthalpies of binding instead of entropies of binding, contrary to what was predicted.[44] There was a correlation of more favorable binding affinities within the ligand series as straight chain alkyl R groups were lengthened from ethyl to pentyl, and as aliphatic ring sizes increased from cyclopropyl to cyclohexyl. The enhancement in binding affinity was found to be due to a more favorable ΔH° of binding, where the ligands with more hydrophobic surface area engaged in more nonpolar contacts. It was predicted that the enhancement in binding affinity would be due to a more favorable ΔS° of binding, which would be a result of desolvation of the ligand and protein to release solvating water molecules to the bulk. These results show that predicting binding thermodynamics is remarkably difficult, and there remains a great deal to be understood about protein-ligand interactions before predictions can be considered useful.

Chapter 2: Design and synthesis of Ligands for the Src SH2 Domain

2.1 INTRODUCTION

The root cause of the observed entropy/enthalpy compensation in the Src studies was hypothesized as being at least in part due to be the alteration of the highly sensitive hydrogen bonds between the pY residue and its binding pocket. This observation led us to query whether preorganizing pYEEI at the pY+3 site would confer favorable binding entropy with either lessened or no enthalpic penalty. Isoleucine, which is the residue at the pY+3 site, bears a hydrocarbon side chain that engages in nonpolar contacts with the protein. Waksman found that substituting Ile for other amino acid residues led to a decrease in binding affinity.[36] Interestingly, Ile had a less favorable $\Delta S°$ of binding, but had a strong $\Delta H°$ of binding relative to the other nonpolar amino acid residues. A highly favorable enthalpy of binding is suggestive of strong nonpolar contacts and given the marked decrease in potency of other amino acids at the pY+3 site, the authors concluded that an Ile residue at the pY+3 site engaged in optimal nonpolar contacts, suggesting the binding site is highly ordered. This conclusion was unusual, since unlike polar binding sites, binding contacts in hydrophobic sites are distance dependent but not angle dependent.

Ligand	K_a (M^{-1})	$\Delta G°$ (kcal mol^{-1})	$\Delta H°$ (kcal mol^{-1})	$-T\Delta S°$ (kcal mol^{-1})
pYEEI	5.5 (±0.7) 10^6	-9.2 ± 0.1	-7.7 ± 0.2	-1.5 ± 0.2
pYEEL	2.3 (±0.4) 10^6	-8.7 ± 0.1	-5.6 ± 0.4	-3.1 ± 0.4
pYEEV	2.2 (±0.3) 10^6	-8.7 ± 0.1	-5.4 ± 0.2	-3.3 ± 0.2
pYEEA	5.7 (±2.0) 10^5	-7.8 ± 0.2	-5.1 ± 0.4	-2.7 ± 0.4
pYEEG	2.6 (±0.1) 10^5	-7.4 ± 0.1	-3.6 ± 0.1	-3.8 ± 0.1

Table 4: Binding data for octapeptides Ac-PQ**pYEEX**IPI binding to Src SH2 domain.[36]

2.2 DESIGN OF SRC SH2 LIGANDS

Given the relative importance and high degree of residue specificity of the pY+3 site for the pYEEI-Src SH2 binding event, we were intrigued by the possibility of preorganizing pYEEI at its pY+3 site. The specificity required of the pY+3 residue of the ligand to achieve potent binding with Src SH2 suggested that introducing a conformational constraint might enhance $\Delta S°$ of binding, perhaps to a significant extent. However, since the binding pocket is nonpolar, we did not expect to see as significant of a loss of enthalpy as was observed in the prior work with Src SH2 ligands.[37] The less favorable $\Delta H°$ of binding with conformational constraints at the pY site was at least in part due to disruption of the hydrogen bonds between the phosphotyrosine and the binding pocket. Hydrogen bonds, as stated earlier, are highly dependent on both distance and angle for strong interactions. By contrast, nonpolar contacts characterize binding in the pY+3 site, which are not angle dependent, but rely only on distance. Assuming the structure of the ligand with the conformational constraint at the pY+3 site places the R group in a conformation that closely mimics the pYEEI ligand, the nonpolar contacts should not weaken much at

all. To this end, we decided to synthesize the constrained ligand **24** and its flexible counterpart **25**. Additional studies were planned for studying the constrained ligand **26** and the flexible control **27**, which will further enhance our understanding of the results of constraining the pYEEI ligand at the pY+3 site.[38,45]

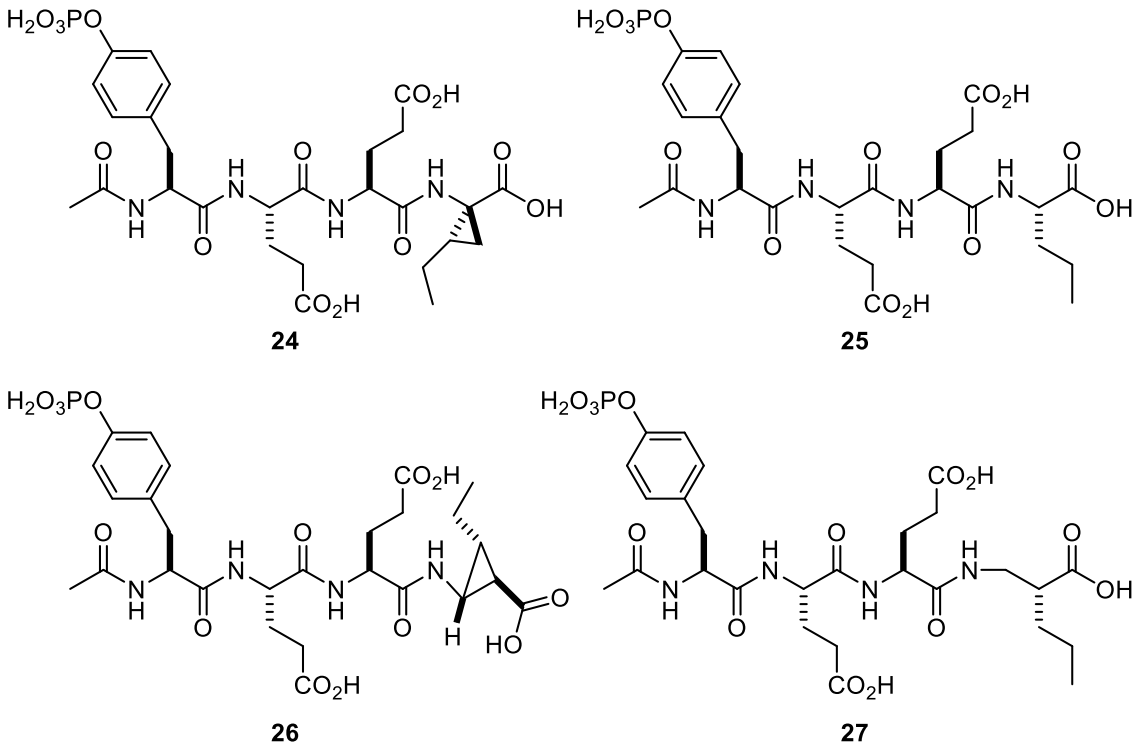

Ligand **24** was designed with the goal of constraining the ethyl group of Ile into its binding conformation in ligand **1** using a cyclopropane ring. The design maintains the same number of heavy atoms as **1**, but the methyl group of **1** becomes the methylene group of **24**. This presents one key difference between ligands **24** and **1**; the methylene group of the cyclopropane does not reside in the same relative space as the methyl group does in Ile. Ligand **27** was designed to permit bond rotation about all carbon-carbon bonds. The

flexible analog will also probe the effect of removing the methyl group from Ile in **1**. The methyl group of Ile in **1** engages in nonpolar contacts with the protein which will not be available for **25** to engage in, adding to the relevance of **24** as an analog.

2.3 SYNTHESIS OF CONSTRAINED LIGAND

The synthesis of **24** commenced with the preparation of the constrained cyclopropyl amino acid **28**. This amino acid is a natural product and has been made several times,[46] but the route reported by Ortuño was selected as the protocol for our synthesis due to its brevity and overall high-yielding steps that confer excellent levels of diastereoselectivity.[46] It should be noted that Schöllkopf also completed the synthesis of **28** by a different route, but a colleague was experiencing difficulties replicating the reported procedure.[47] Hence, we decided to explore the Ortuño route to **28**, but we discovered it too was not without problems.

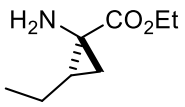

28

One of the key steps for preparing *allo*-coronamic acid (**28**) in the Ortuño synthesis was a Horner-Wadsworth Emmons (HWE) reaction between (D)-glyceraldehyde acetonide **29** and the phosphonate **32** (Scheme 1). Ortuño prepared known compound **32** in three steps following literature precedent (Scheme 2).[48,49] The resulting olefinic amino acid **40** was treated with diazomethane and light to introduce the cyclopropane with complete diastereomeric control in quantitative yield to provide cyclopropyl amino acid **41** (Scheme 1). The acetonide was deprotected to reveal the diol, which was then converted to the vinyl

cyclopropane **45** over three steps in good yield. Hydrogenation of the vinylcyclopropane provided the methyl ester of *allo*-coronamic acid, which we would use to begin the sequence of peptide couplings to furnish tetrapeptide **24**.

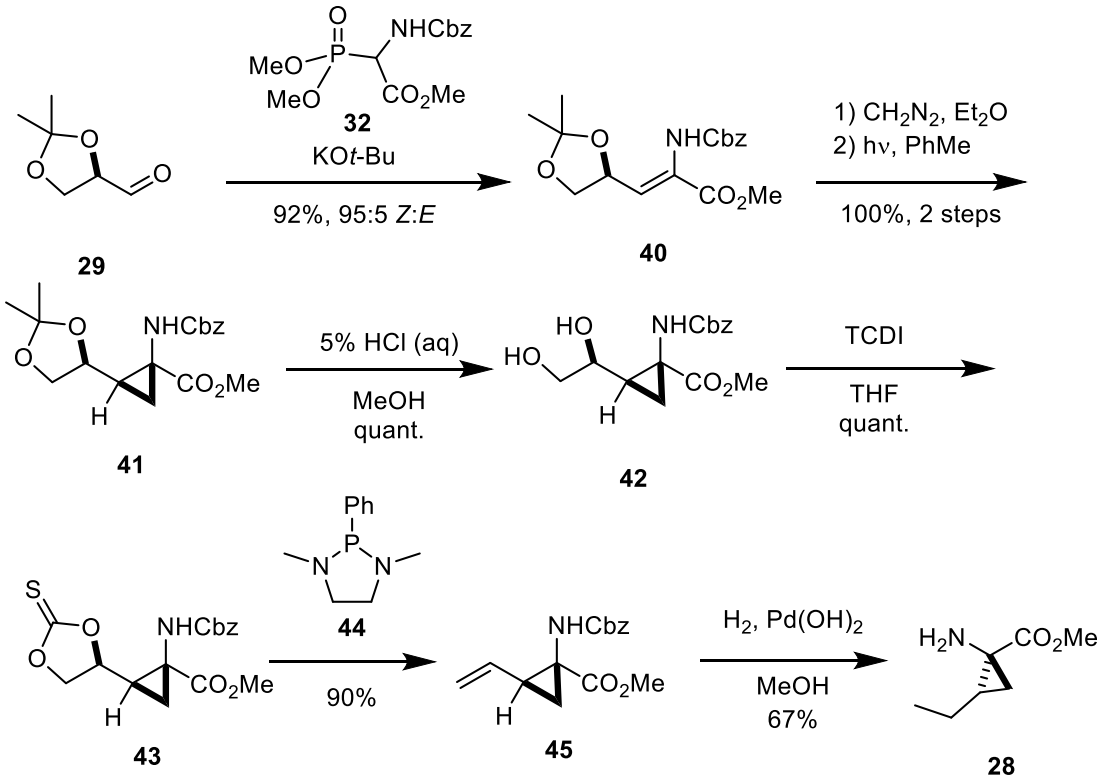

Scheme 1: Ortuño route to *allo*-coronamic acid (**28**).[46]

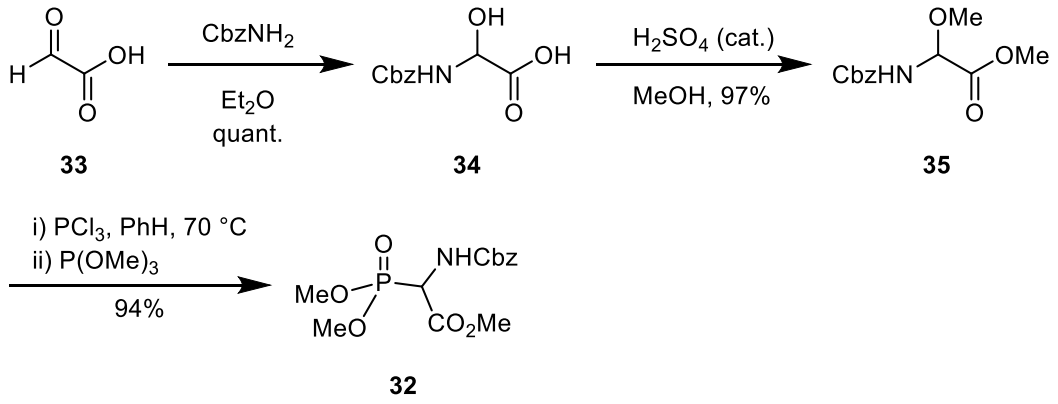

Scheme 2: Ortuño protocol for preparing α-phosphonoglycinate **32**.[46]

Though commercially available, D-glyceraldehyde acetonide (**29**) is somewhat costly, but it is readily prepared from inexpensive D-mannitol (**30**) (Scheme 3). This known two-step process was achieved by first selectively protecting **30** as the 1,2;5,6 *O*-isopropylidine acetal **31**,[50] which afforded **29** upon oxidative cleavage in 59% yield over two steps.[51]

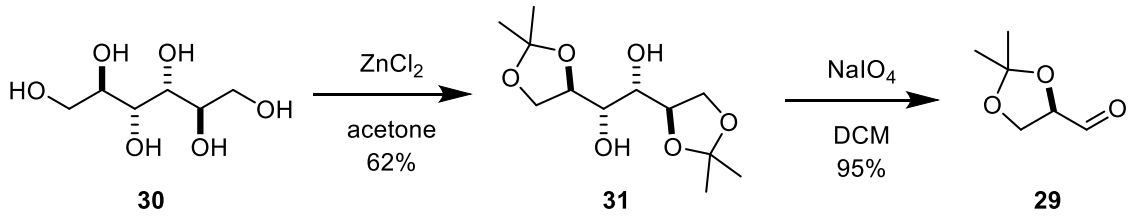

Scheme 3: Synthesis of glyceraldehyde acetonide **29**.

Although the synthesis of **29** was achieved without complication, the preparation of the phosphonate **32** proved more troublesome. Ortuño prepared the phosphonate via an

Arbuzov reaction of trimethyl phosphite with the α-haloglycinate **38**. Toward the preparation of **32**, the α-hydroxy glycine **34** was first formed from the reaction of benzyl carbamate with glyoxylic acid (**33**) (Scheme 4).[52] Conversion of **34** to the methyl ester **35** was achieved under acidic conditions in methanol. We were dissatisfied with the low yield to give **34**, so a different protocol to form the phosphonate **32** was investigated.

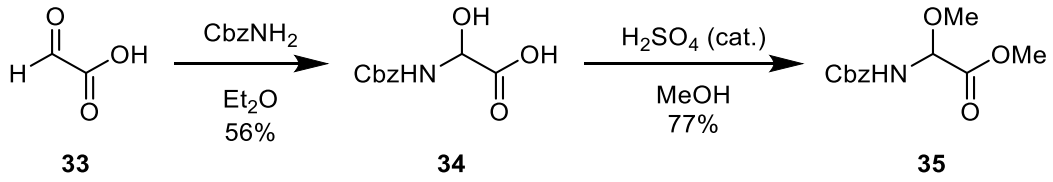

33 **34** **35**

Scheme 4: Abandoned partial route to phosphonate **32**.

Instead of constructing the methyl ester from a carboxylic acid, we turned to forming methyl glyoxylate (**37**) through periodic acid-mediated oxidative cleavage of dimethyl tartrate **36** (Scheme 5).[53] Methyl glyoxylate (**37**) was allowed to react with benzyl carbamate in the presence of acetyl chloride and a catalytic amount of acetic acid to furnish the α-chloroglycinate **38**.[54] It had been reported that **38** is isolable upon evaporation of the solvent,[54] but it readily undergoes hydrolysis on silica gel. Accordingly, we decided to isolate **38** and use it in the following reaction without purification. Unfortunately, a mixture (50:50) of α-chloro- and α-acetoxyglycinates **38** and **39** (determined by ^{1}H NMR) was produced. Due to the difficulty of separating **38** and **39**, the mixture was treated with

phosphorus trichloride to effect complete conversion to the α-chloroglycinate **38** in 62% yield.

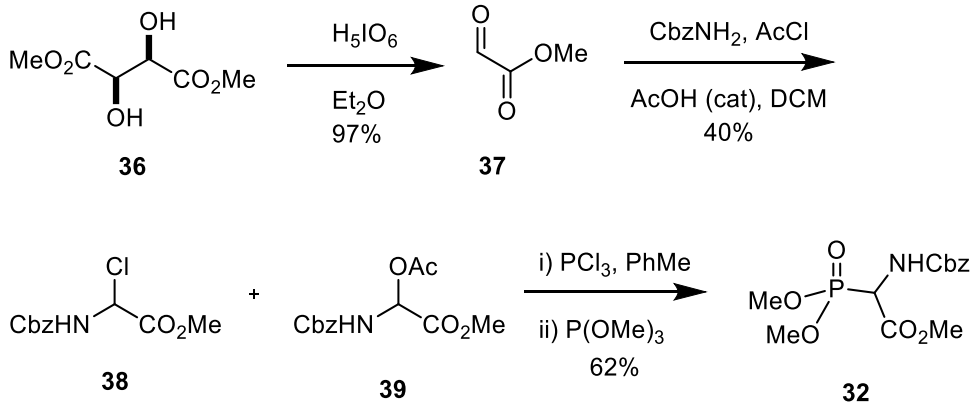

Scheme 5: Synthesis of phosphonate **32**.

Frustrated by the inability to isolate **38** cleanly and efficiently, we hypothesized that the introduction of trimethyl phosphite to the reaction could initiate the Arbuzov reaction without isolating the glycinate **38**. We modified the reaction conditions for the formation of **38** by using toluene instead of dichloromethane in order to accommodate the higher reaction temperatures required for the Arbuzov reaction. Benzyl carbamate, methyl glyoxylate, and AcCl were stirred overnight according to the original report to prepare **38**, and then $P(OMe)_3$ was added, and the mixture was stirred for 3 h. To our delight, phosphonate **32** was formed by this 4-component-one-pot reaction in 60% yield (Scheme 6).[54,55]

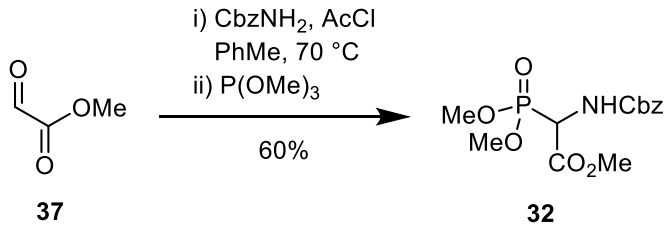

37 **32**

Scheme 6: One-pot reaction from **37** to **32**.

With both **29** and **32** in hand, the HWE reaction proceeded smoothly to give **40** (Scheme 7), albeit in only 56% yield.[46,49] Ortuño obtained **40** in 92% yield and 95:5 *Z*:*E* ratio. While we were able to reproduce the high stereocontrol, the reported yield could not be replicated.

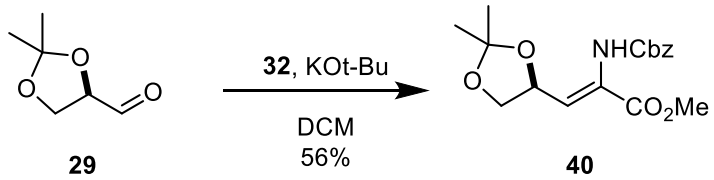

29 **40**

Scheme 7: HWE reaction between **29** and **32**.

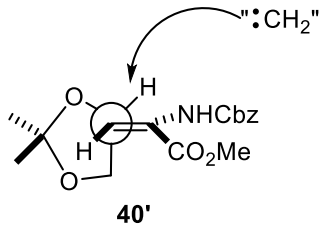

40'

Figure 6: Felkin-Ahn model of **40**.

The olefinic amino acid **40** is the substrate for a cyclopropanation reaction, which Ortuño accomplished via a [2+3] cycloaddition between the olefin in **40** and diazomethane followed by extrusion of dinitrogen. In the interest in not using such a dangerous reagent, alternative methods to cyclopropanate the olefin were explored. At this juncture, we faced perhaps the greatest question of our modified synthesis: What is the facial selectivity of alternative cyclopropanation methods? Ortuño achieved high diastereoselectivity (95:5 *Z*:*E*) and invoked the Felkin-Anh model (e.g., **40'**) of the transition state to rationalize the observed outcome. Based upon this model, we had reason to believe that other cyclopropanation reactions would also be diastereoselective (Figure 6). One alternative that was considered included using the less-explosive (trimethylsilyl)diazomethane in the same manner. This reagent is not particularly desirable, as it is highly toxic and the tendency to explode is merely mitigated compared to diazomethane. Furthermore, a reaction with (trimethylsilyl)diazomethane would necessitate an additional step to remove the TMS group on the resulting cyclopropane ring. A Corey-Chaykovsky cyclopropanation was also briefly considered, but such cyclopropanations typically require good Michael acceptors; the partial enamine character of **40** gave us pause. We then surmised that a Simmons-Smith reaction (or one of the several modifications) might serve as an effective reaction and was explored first.

The Simmons-Smith reaction has been known for several decades, and it may be applied to a wide variety of alkenes. Moreover, the reaction is chemoselective and has high functional group tolerance.[56] A particularly attractive feature of the Simmons-Smith reaction is that the reaction can be rendered stereoselective through the use of a directing

group like an allylic alcohol or ether, the latter of which is a moiety present in **40**.[56] We anticipated high stereoselectivity since the most stable conformation of the substrate placed the allylic oxygen in position to direct the active zinc species to the appropriate face (Figure 6).

The original Simmons-Smith reaction employs a Zn/Cu couple, which is troublesome to prepare, provides inconsistent results, and is often lower-yielding than some of the modern modifications.[56] The Furukawa[58] and the Denmark modifications[59] are two of the most commonly utilized variations. Both of these reactions employ Et_2Zn as the zinc source but differ in the carbenoid source; the Furukawa modification uses CH_2I_2 whereas Denmark conditions use CH_2ICl. There are also other alternatives wherein the reactivity of the zinc carbenoid is modulated by the identity of the carbenoid. For example, the Shi modification employs a trifluoromethylacyl carbenoid that is highly reactive,[60] and the Charette modification uses a di-*n*-butylphosphonate-derived organozinc species that is less reactive.[61] We opted to test the Furukawa conditions first, due to the availability of diiodomethane and the success of this particular modification in related substrates.[56,62] Indeed, the cyclopropanation using the Furukawa modification provided **41** in 90% yield and >20:1 dr (Scheme 8).[62] The ^{1}H NMR spectrum of **41** matched the correct diastereomer as reported in the literature.[46] Deprotection of the acetonide **41** to the diol **42** proceeded smoothly in 98% yield.

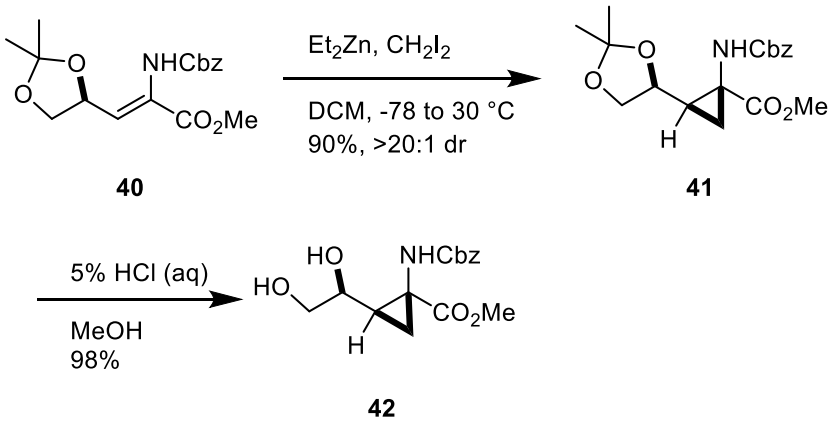

Scheme 8: Cyclopropanation and acetonide hydrolysis.

We initially planned to elaborate the diol **42** via a Corey-Winter olefination.[46] To this end, **42** was quantitatively converted to the thiocarbonate **43** with 1,1-thiocarbonyldiimidazole (TCDI) (Scheme 9).

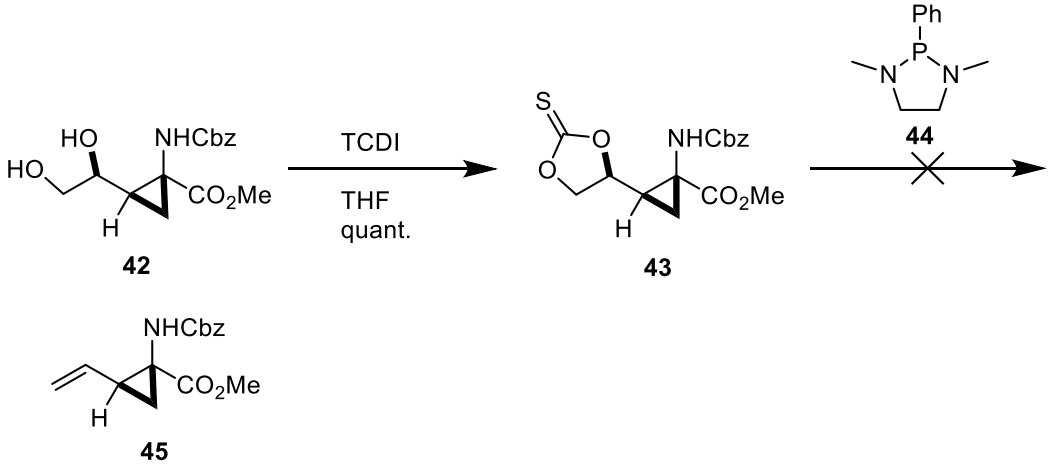

Scheme 9: Conversion of the diol moiety to the saturated alkyl chain.

The thiocarbonate **43** was stirred with the Corey-Hopkins reagent **44**,[63] a phosphine that eliminates the thiocarbonate under milder conditions than the original Corey-Winter protocol.[64] Unfortunately, the desired olefin **45** could not be isolated, and the inconvenience of using the air and moisture-sensitive TCDI and Corey-Hopkins reagent helped to persuade us to find a new approach to the elaboration of diol **42** to the amino acid **28**. Radical-based deoxygenations were not explored since carbon-centered radicals adjacent to cyclopropane rings readily undergo ring-opening reactions, so we turned to a two-step oxidative cleavage and Wittig olefination procedure to convert **42** to **28**.

Diol **42** was subjected to a periodate-mediated oxidative cleavage to give the aldehyde **53** (Scheme 10).[46] The aldehyde **53** was used directly without purification in the next reaction to avoid possible epimerization. Olefination of **53** with the lithium ylide of methyl(triphenyl)phosphonium bromide gave varying yields (40-60%, two steps) of the vinylcyclopropane **45**. According to the protocol reported by Ortuño, the alkene moiety of **45** could be reduced with concomitant removal of the Cbz protecting group in one operation by catalytic hydrogenation with Pearlman's catalyst. Unfortunately, we were not able to replicate this reduction, and none of the desired **28** could be identified.

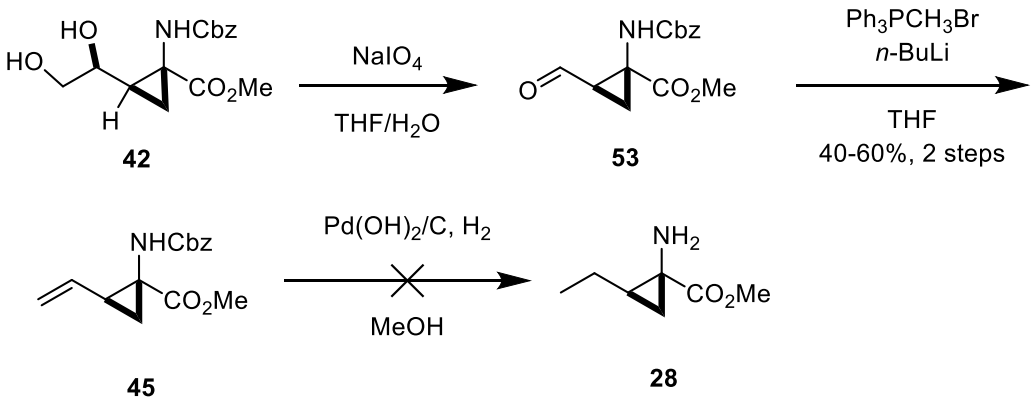

Scheme 10: Alternative protocol for the transformation of diol **42** to cyclopropyl amino acid **28**.

Due to the various problems with the Ortuño approach to **28**, this route was abandoned in favor of the Schöllkopf approach. The problems associated with reproducing the Schöllkopf approach were solved by a colleague during the exploration of the Ortuño route as an alternative strategy. This route to **28** uses the eponymous "Schöllkopf auxiliary." This auxiliary is a protected cyclic dipeptide consisting of a bulky amino acid such as valine or *t*-butylglycine and glycine, which becomes the amino acid backbone of the desired compound. Deprotonation of the glycine moiety and subsequent treatment with an electrophile is rendered diastereoselective by the chiral center of the valine moiety. The newly synthesized enantioenriched amino acid can be liberated from the auxiliary by acidic hydrolysis.

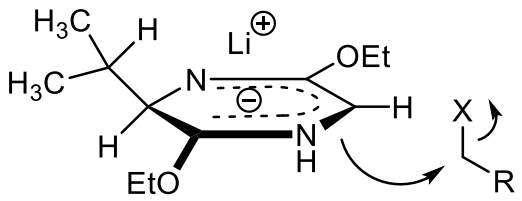

Figure 7: Stereochemical model of Schöllkopf asymmetric amino acid synthesis. Depicted with D-valine as the auxiliary.

The synthesis of **28** following the procedure reported by Schöllkopf began with the protection of D-valine and subsequent coupling with ethyl glycinate to form **48** in 87% yield over two steps (Scheme 11).[65] Heating the dipeptide **48** under reflux in 1,2-dichlorobenzene gave the diketopiperazine **49** in 74% yield. Alkylation of **49** with ethyl Meerwein's salt provided the bislactim ether **50** in 77% yield, which was then deprotonated with *n*-BuLi and alkylated with 1,4-dichloro-*trans*-2-butene to give **51** in 55% yield. Reacting **51** with *n*-BuLi furnished the cyclopropyl spirocycle **52** via an intramolecular S_N2' reaction in 40% yield, and subsequent diimide reduction of the terminal olefin delivered **53** in 91% yield. Acid promoted hydrolysis of **53** liberated the cyclopropyl amino acid ester **28** from valine ethyl ester.

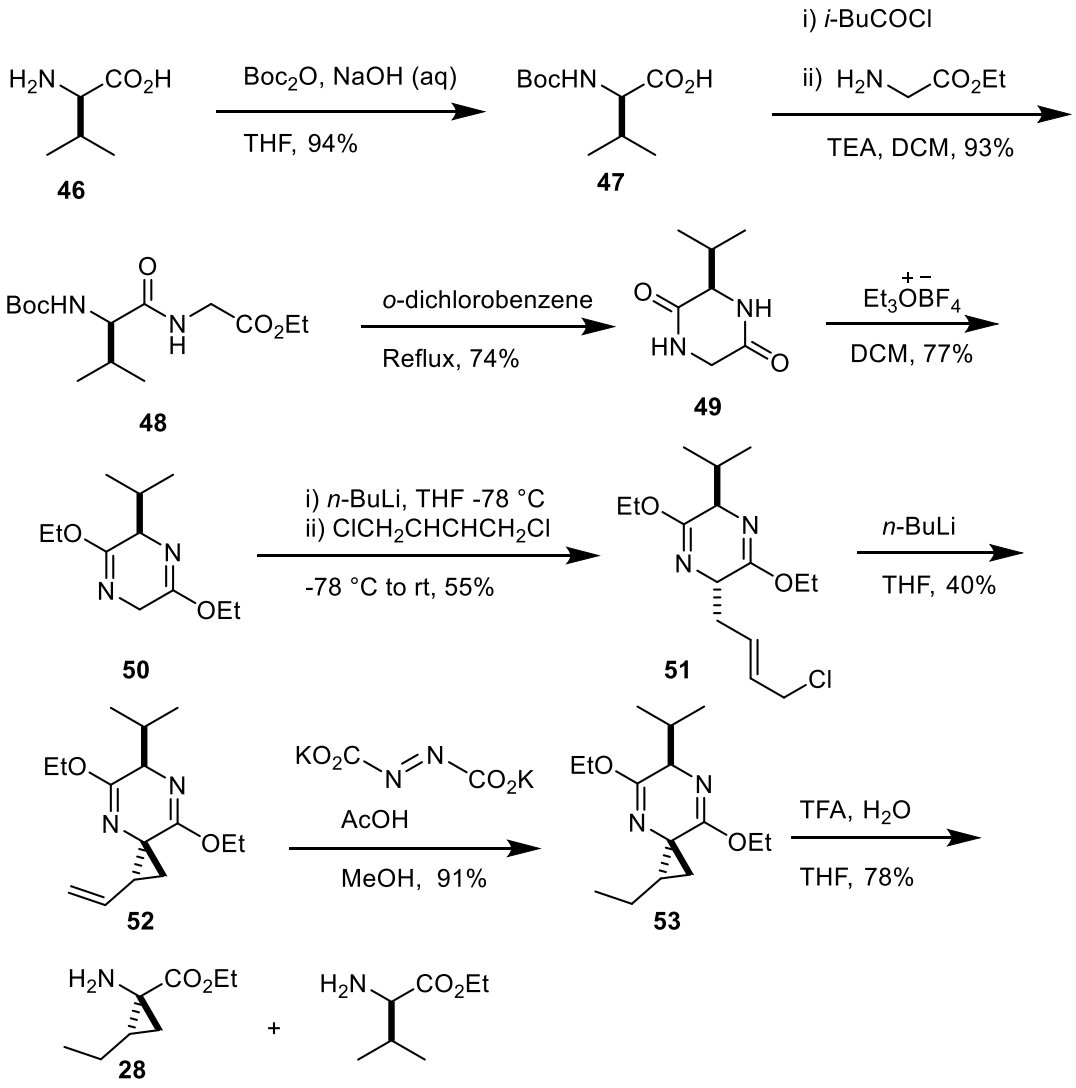

Scheme 11: Synthesis of the Schöllkopf auxiliary and formation of cyclopropyl amino acid **28**.

Elaboration of amino acid **28** to the constrained ligand **24** began with coupling **28** to the protected glutamate **54** to provide dipeptide **55** in 51% yield (Scheme 12). An X-ray crystal structure was obtained for this compound in order to confirm the absolute stereochemistry of the cyclopropyl amino acid (Figure 8). Boc deprotection of the dipeptide **55** followed by peptide coupling with another protected glutamate **54** delivered the tripeptide **57** in 71% yield over two steps. Boc deprotection of **57** followed by coupling with protected phosphotyrosine **59** provided the fully protected tetrapeptide **60**. A global deprotection of **60** appeared unlikely given the presence of an ethyl ester among the relatively labile benzyl esters and benzyl carbamate. Accordingly, the benzyl carboxylic esters, benzyl phosphate esters, and benzyl carbamate were removed by hydrogenolysis to provide **61**, which was saponified and then acylated to provide the final ligand **24** (Scheme 13). The final two steps proceeded in 17% yield after HPLC purification.

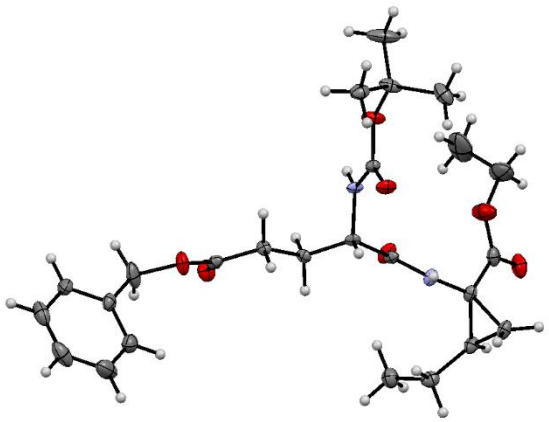

Figure 8: X-ray crystal structure of dipeptide **55**.

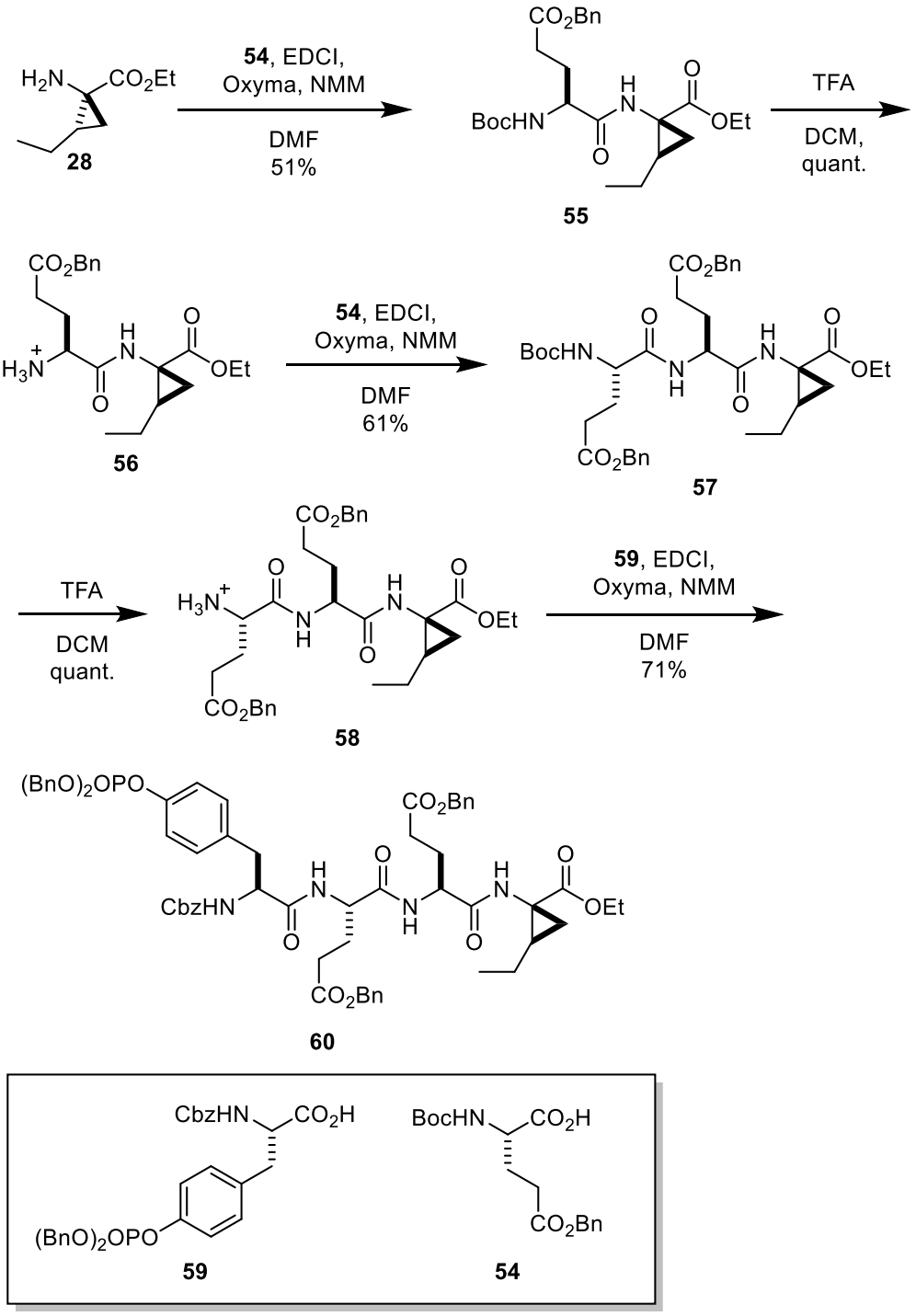

Scheme 12: Synthesis of tetrapeptide intermediate **60**.

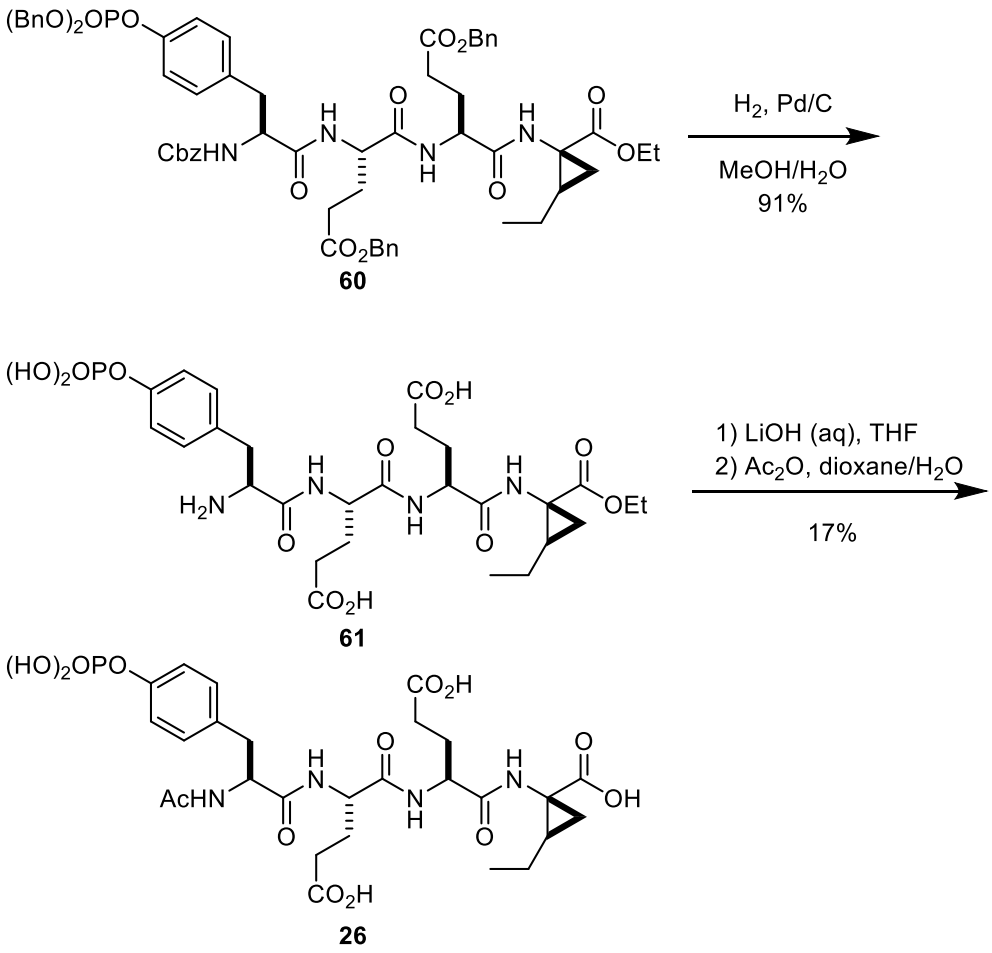

Scheme 13: Completion of constrained ligand synthesis.

2.4 SYNTHESIS OF FLEXIBLE LIGAND

The synthesis of the flexible ligand **25** commenced with the Fischer esterification of commercially available L-norvaline (**63**) with benzyl alcohol (Scheme 14),[68] as described by Dr. Amy Bonaparte.[45] The *p*-toluenesulfonic acid salt of L-norvaline benzyl ester **64**, which was isolated in 80% yield, was subjected to a peptide coupling with the protected glutamate **54** to provide the dipeptide **65** in 85% yield. Following the quantitative deprotection of **65**, amine **66** was subjected to another peptide coupling with **54** to furnish

the tripeptide **67** in 80% yield. The tripeptide was deprotected to give **68**, which was coupled with phosphotyrosine **59** to provide the protected tetrapeptide **69**. Following global deprotection by hydrogenolysis, the crude tetrapeptide **70** was acylated to afford the final ligand **25** (Scheme 15).

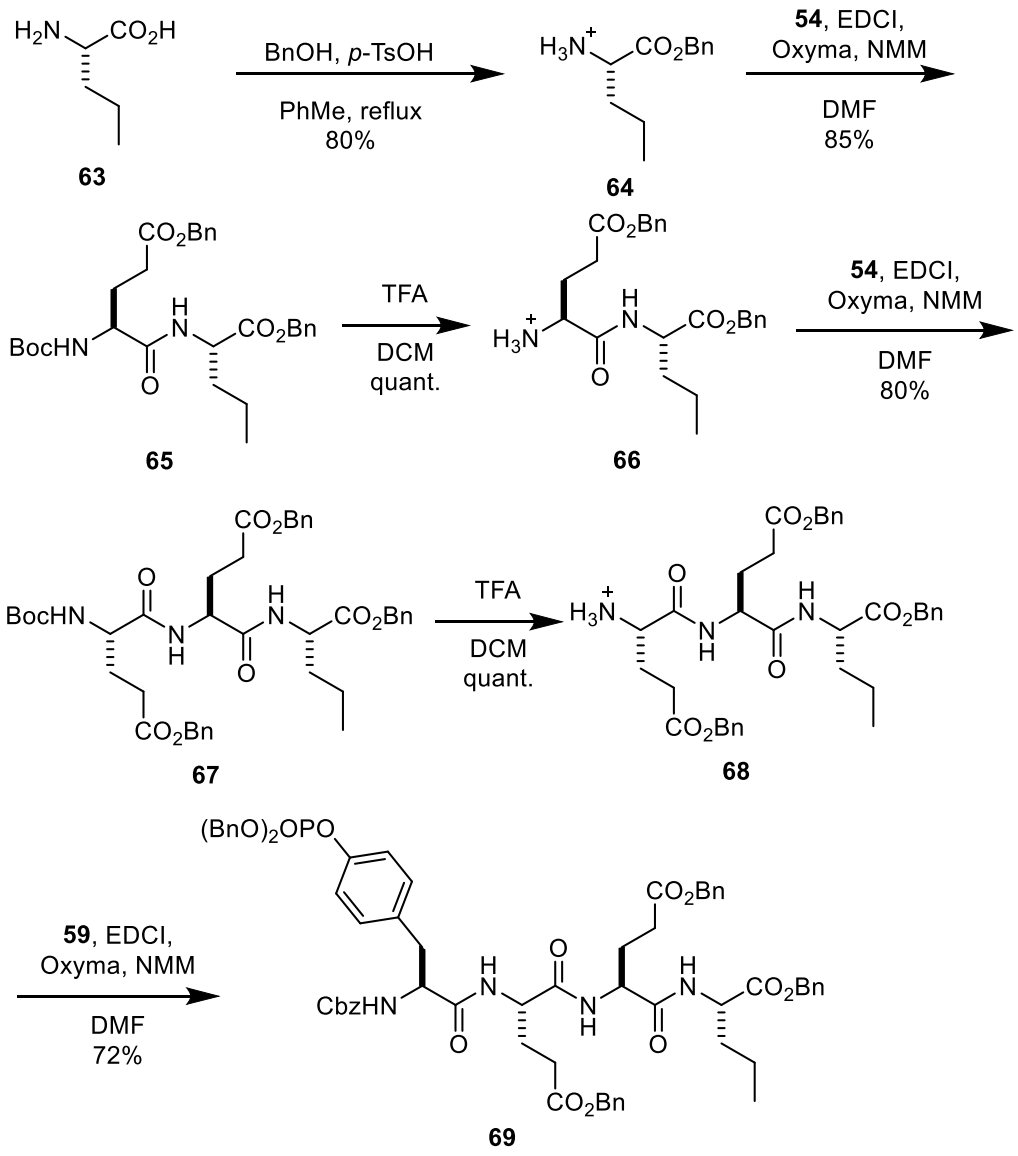

Scheme 14: Synthesis of tetrapeptide intermediate **69**.

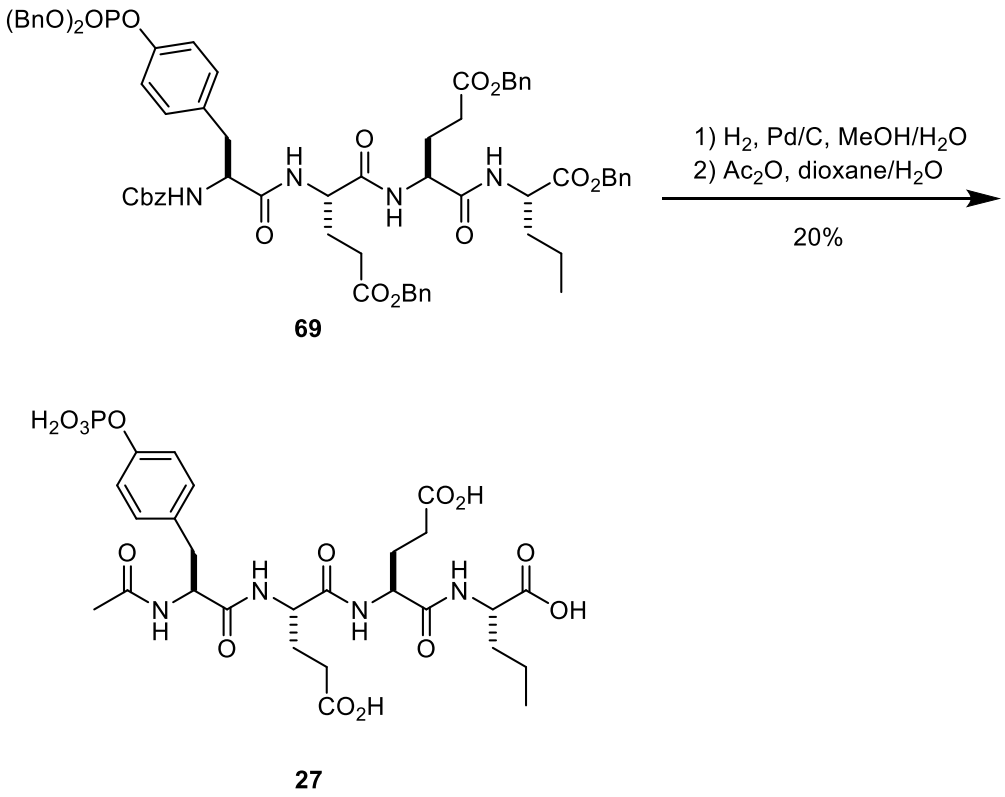

Scheme 15: Completion of flexible ligand synthesis.

2.5 ITC STUDIES

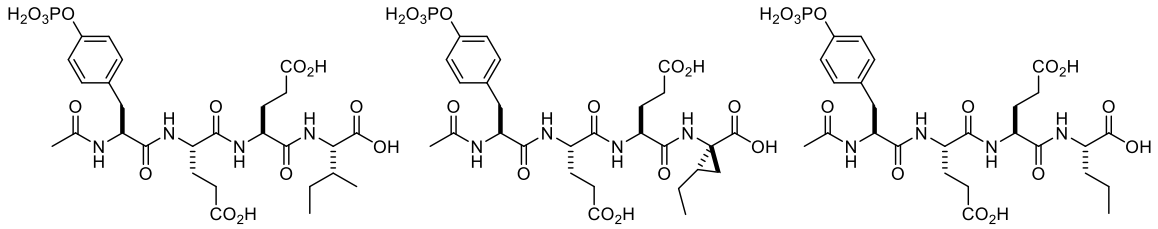

1 24 25

Ligand	K_a (M^{-1})	$\Delta G°$ (kcal mol^{-1})	$\Delta H°$ (kcal mol^{-1})	$T\Delta S°$ (kcal mol^{-1})
1 (lit)[37]	4.1 (± 0.1) 10^6	-9.01 ± 0.01	-6.06 ± 0.05	-2.95 ± 0.07
1	4.2 (± 0.3) 10^6	-9.03 ± 0.05	-5.15 ± 0.25	-3.89 ± 0.64
24	1.5 x 10^6	-8.43	-5.30	-3.13
25	4.0 (± 0.3) 10^6	-9.00 ± 0.05	-5.36 ± 0.34	-3.64 ± 0.66

Table 5: Binding data for ligands **1**, **24**, and **25** binding to Src SH2 domain.

ITC studies were performed on ligands **24**, **25**, and compared to pYEEI (**1**). We first performed binding studies of **1** with the Src SH2 domain. We found that the K_a and $\Delta G°$ values were in good agreement with the previous report (Table 5),[37] but there was a difference in $\Delta H°$ and $\Delta S°$ between the experiments. It is not clear what caused the disparity in results, though there are a few possible reasons. Since the original data were obtained over 15 years ago, the isothermal titration calorimeter had been replaced. Additionally, the instrument was malfunctioning and required changing titration conditions from the settings used in the original report to obtain reproducible data. In particular, baseline noise from the instrument was an issue when the calorimeter stirred at the rate in which previous Martin group ITC experiments had been run. The stir rate was lowered

and the time between ligand injections to the protein was increased to ensure good mixing. There were also problems with baseline drift which required a lengthy delay (~1.5-2h) between the start of data collection and the first injection. Both the baseline drift and background noise issues were alleviated when the power setting for the ITC was lowered. The power setting was within normal bounds prescribed by the instrument manual and should not have affected the values attained. It is also noteworthy that the standard errors are larger for current experiments compared to the prior report, though they are acceptable. Despite all these changes, the data obtained were reproducible and the reported values are the average of triplicate trials for **1** and quadruplicate trials for **25**.

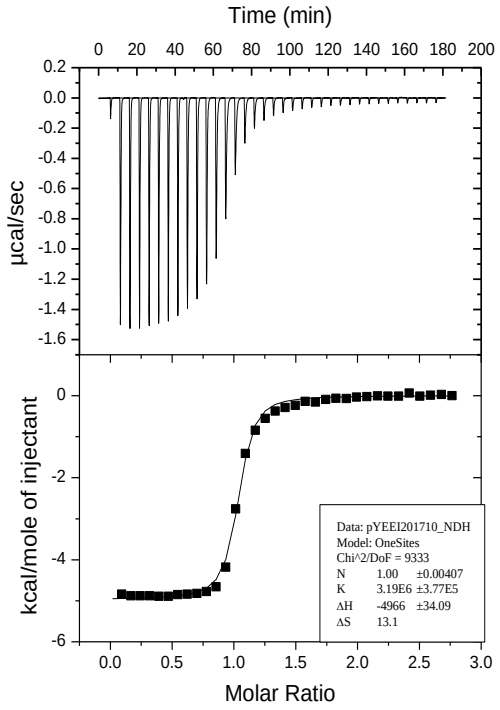

Figure 9: Example ITC trace of **1**.

Top: Raw data as heats of complexation (µcal/sec).
Bottom: Integrated ITC data as heats of binding per mol of ligand.

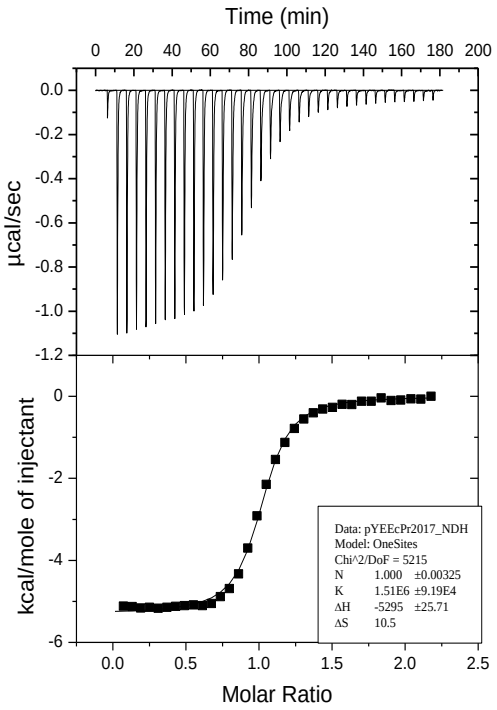

Figure 10: Example ITC trace of **24**.

Top: Raw data as heats of complexation (µcal/sec).
Bottom: Integrated ITC data as heats of binding per mol of ligand.

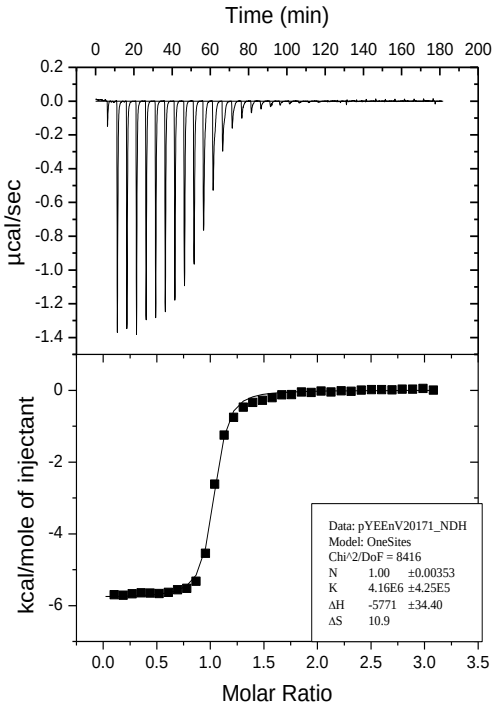

Figure 11: Example ITC trace of **25**.

Top: Raw data as heats of complexation (µcal/sec).
Bottom: Integrated ITC data as heats of binding per mol of ligand.

While it was worrisome that $\Delta H°$ and $\Delta S°$ values attained for **1** were not in close agreement with the prior report, even when considering the margins of error of the present binding experiments, we would still be able to test our hypothesis: Does preorganizing the ligand at the pY+3 site enhance binding affinity over a non-modified ligand, and if so, is it due to a more favorable $\Delta S°$ of binding?

We first tested the flexible ligand **25** and found that it bound with a comparable K_a and $\Delta G°$ as **1**, but it bound with a less favorable $\Delta S°$ and more favorable $\Delta H°$ (Table 5). The data did fall within the margins of error for both ligands, however. Recall that pY+3 mutagenesis studies by Waksman (Table 4) revealed that the pY+3 = Ile ligand bound with a significantly higher $\Delta H°$ than leucine, valine, alanine, and glycine residues, whereas it had a much less favorable $\Delta S°$ of binding. Thus, it is surprising that we would observe a more favorable $\Delta H°$ of binding for ligand **25** accompanied by a less favorable entropic component. Waksman proposed that the highly favorable $\Delta H°$ of binding for the isoleucyl ligand and relatively low corresponding $\Delta S°$ value indicated a strong specificity for Ile and that it maximized van der Waals contacts while other ligands apparently did not. The norvaline residue of ligand **27** lacks a methyl group that isoleucine has, which is somewhat confounding considering the lack of a methyl group would be predicted to have fewer van der Waals contacts thereby have a less favorable enthalpy of binding. What is interesting, though, is that **1** and **25** are equipotent and have similar $\Delta S°$ and $\Delta H°$ values of binding; in Waksman's study altering pY+3 from isoleucine to other nonpolar amino acids he observed a twofold decrease in binding affinity when the isoleucine residue was converted to a leucine or valine residue. It may be the case that a propyl group in the pY+3 side chain fits

intimately in the binding pocket, whereas an isobutyl group (leucine) is too large. On the other hand, valine, with the comparatively smaller R group, is unable to occupy the binding pocket as deeply. The β-branched methyl group of the valine side chain, however, is likely important to binding since the valyl and leucyl analogs of Waksman's ligands were equipotent with each other and had similar entropies and enthalpies of binding.

Our result with the norvaline residue implies that a straight chain occupying the binding pocket is more impactful on $\Delta H°$ of binding than the β-methyl moiety of isoleucine. Perhaps the β-methyl group of isoleucine blocks the rest of the side chain from binding as deeply within the binding site as the norvaline residue. If this characterization of the isoleucine methyl group as a steric block for binding is correct, then that could potentially rationalize the less favorable $\Delta S°$ of binding observed in ligand **25** wherein the closer association of the norvaline residue is more ordered by nature of having stronger van der Waals interactions.

Ligand **24** has only been tested once at the present time; accordingly, any discussion will naturally be limited by the lack of replication. We found that **24** had a slightly lower K_a and $\Delta G°$ as compared to ligand **1**, and like ligand **25** it bound with a more favorable $\Delta H°$ of binding and a less favorable $\Delta S°$ of binding than ligand **1** (Figure 7). We were surprised that our hypothesis that ligand **24** would not only bind more strongly but have a less favorable entropy of binding was completely backwards. It is worth noting that the predicted ground state conformation of **1** at the pY+3 site corresponds to the bound conformation of that residue. In other words, the Ile group in **1** is already preorganized in its binding conformation in the solution state. What is also striking is that **24** and **25** had

nearly the same $\Delta H°$ of binding; ligand **24** was less potent than **25** solely due to a less favorable $\Delta S°$ of binding.

The preorganized ligand **24** has the same number of carbon atoms as **1**, but it has a methylene group instead of a methyl group on the side chain of the pY+3 residue. The geometry of the cyclopropane invariably alters the position of the methylene group such that it does not approximate the methyl group of the isoleucine residue in **1**. As previously mentioned, it is possible that the β-branched methyl group is not very important for potent binding and that the presence of a non-branched alkyl chain that binds deeply within the binding pocket is more important. Therefore, it might be the case that the cyclopropylethyl side chain can bind deeply within the nonpolar binding site since the β-methylene group in **24** cannot be positioned where the β-methyl group of **1** resides. The implications of this constraint on the conformation are unclear without structural data to study the ligand binding mode and the interactions in the complex.

We also know that ligand **24** is less potent than **25**, solely due to a less favorable $\Delta S°$ of binding. The obvious first conclusion would be that ligand **24** does not approximate the binding conformation of **25**. The key structural difference between **24** and **25** is that ligand **24** has an extra methylene group, which not only adds hydrophobic surface area, but restricts the degrees of freedom of the R group. What is not clear is how that structural difference manifests in the binding conformations with the protein. The rigidity imparted by this structural feature may force the constrained ligand to adopt a conformation in solution that does not resemble its binding conformation, and furthermore might restrict any bond rotations required for the ligand to adopt the binding conformation.

2.6 SUMMARY AND FUTURE DIRECTIONS

Predicting the thermodynamic effects of preorganizing ligands for protein binding by introducing conformational constraints is difficult and does not always lead to the expected results. Herein we explored the effects of preorganizing the pYEEI ligand at the pY+3 site using a cyclopropane ring as a conformational constraint. Previous Martin group reports revealed that constraining the pY residue of ligand **1** enhanced binding affinity to the Src SH2 domain through a more favorable $\Delta S°$ of binding, as predicted. However, the more favorable $\Delta S°$ of binding was offset by a less favorable $\Delta H°$ of binding. Since the pY binding pocket is characterized by hydrogen bonds, which are sensitive to distance and angle between polar contacts, even small perturbations in the conformations of the ligands resulted in significant changes to the thermodynamics of binding. As mentioned in Section 1.52, however, preorganizing the pY residue of the pYVN ligands for Grb2 SH2 domain binding led to a less favorable $\Delta S°$ of binding accompanied by a more favorable $\Delta H°$ of binding.

We designed ligands **24**-**27** to test our hypothesis that introducing a conformational constraint at the nonpolar pY+3 residue would enhance binding affinity through a more favorable $\Delta S°$ of binding as was observed with ligand **2** while mitigating the entropy-enthalpy compensation since van der Waals contacts are only dependent on distance, not angle. Ligand **25** was prepared in eight steps and ligand **24** was prepared in 16 steps. Intermediate **28**, *allo*-coronamic acid, proved difficult to access. Initial attempts to prepare **28** following the procedure reported by Ortuño, was unsuccessful. During attempts to overcome challenging steps in the Ortuño route, we developed a four-component-one-pot

protocol for preparing α-phosphonoglycinate **32** and avoided the use of diazomethane as a cyclopropanating reagent by employing a variant of the Simmons-Smith reaction. Amino acid **28** was eventually prepared in eight steps using Schöllkopf's procedure, which enabled the preparation of **24** in eight additional steps.

ITC studies revealed that the flexible analog **25** was equipotent with the "native" ligand **1**, though **25** had a slightly more favorable $\Delta H°$ of binding that was offset by a less favorable $\Delta S°$ of binding. This demonstrates another example of entropy-enthalpy compensation, yet it remains unclear what could be the cause of the difference in binding energetics. The entropy and enthalpies of binding of those two ligands are within margins of error, however, so it is difficult to draw definitive conclusions about the differences between **1** and **25**. Constrained ligand **24** was less potent than both **25** and **1**. Surprisingly, ligand **24** had a less favorable $\Delta S°$ of binding than ligand **25**, which is the opposite result we expected to observe.

Structural analysis such as X-ray structures of the protein-ligand complexes will be valuable for contextualizing the ITC results with the binding conformations. Understanding why changing the pY+3 residue from isoleucine to norvaline led to a more favorable enthalpy of binding and less favorable entropy of binding when ligands with leucine and valine residues at the pY+3 site led to a decrease in binding affinity and more favorable entropy of binding will be interesting. If X-ray structures indicate the hypothesis that the β-methyl group of isoleucine prevents deeper insertion of the ligand into the binding pocket is plausible, then preparing other ligands with linear alkyl chains at the pY+3 amino acid side chain may lead to an even more favorable $\Delta H°$ of binding compared

to ligand **25**. Of course, the more favorable $\Delta H°$ of binding of ligand **25** was offset by a less favorable $\Delta S°$ of binding. Nonetheless, this experiment could at least inform how side chain length at the pY+3 site influences the thermodynamics of binding. A crystal structure of Src SH2-bound ligand **24** will also shed light on how altering the backbone geometry of the ligand by introducing the cyclopropane affected the binding conformation and what binding contacts are present that led to a nearly identical $\Delta H°$ of binding as ligand **25**. Molecular dynamics simulations could also prove valuable in analyzing the ligands in their solution state. The result that ligand **24** is a less potent ligand than ligand **25** could be potentially explained by analyzing their solution state energies, as previously mentioned.

Working toward understanding the energetics of protein-ligand interactions is a difficult, but important endeavor. Studies in this arena of science illuminate the complexities of protein-ligand interactions that are key to innumerable biological processes. The more we learn about these interactions, the more we can begin to predict the effects of structure on energetics of binding. The emergence of better models for predicting the effects of small molecule structure on binding will have tremendous impacts in science, but there remains much to study and investigate in the field of protein-ligand interactions.

Chapter 3: Methods and Experimental Procedures

3.1 Organic Synthesis

3.1.1 General

Solvents and reagents were reagent grade and were used without purification, unless otherwise noted. Tetrahydrofuran (THF) and diethyl ether (Et_2O) were dried by passage through two columns of activated neutral alumina. Methanol (MeOH) and *N*, *N*-dimethylformamide (DMF) were dried by passage through two columns of activated molecular sieves. Toluene was dried by passage through a column of activated neutral alumina followed by passage through a column of Q5 reactant. Reactions involving air- or moisture-sensitive reagents or intermediates were performed under either an atmosphere of argon or nitrogen. All glassware used in the reactions was either flame dried or oven dried prior to use. Removal of solvent or volatiles was performed using a rotary evaporator. Thin layer chromatography (TLC) was performed on glass-backed pre-coated silica gel plates (0.25 mm thick with 60 F_{254} indicator) and was visualized by one or more of the following: UV (254 nm) irradiation, treatment with aqueous potassium permanganate ($KMnO_4$) followed by heating, or treatment with aqueous ceric ammonium molybdate (CAM) followed by heating. Flash chromatography was performed with the indicated solvents using silica gel (Silicycle, 40-63 μm, 60 Å). Reverse phase HPLC was performed using a binary solvent system, where solvent A was 0.1% aqueous trifluoroacetic acid (TFA) and solvent B was 0.1% TFA in acetonitrile, with a C18 column (10 mm particle size, 300 Å pore size), 22 mm diameter x 250 mm (flow rate of 5 mL/min). Proton (^1H) and carbon (^{13}C) nuclear magnetic resonance (NMR) were obtained as solutions in the indicated solvents using either a 400 MHz or 600 MHz spectrometer. Chemical shifts are reported in parts per million (ppm, δ) downfield from TMS (δ = 0.00 ppm) and referenced

relative to the 7.24 ppm resonance of $CDCl_3$ or the center of the 2.50 ppm quintet resonance of DMSO-d_6 for ^1H and relative to the center of the triplet of $CDCl_3$ at 77.0 ppm or the center of the 39.5 ppm septet resonance of DMSO-d_6 for ^{13}C. Coupling constants are reported in hertz (Hz). Splitting patterns are designated as: s = singlet; d = doublet; dd = doublet of doublet; ddd = doublet of doublet of doublets; t = triplet; q = quartet; p = pentuplet; m = multiplet; comp = overlapping multiplets of non-magnetically equivalent protons; br = broad; app = apparent.

Schöllkopf auxiliary **50** was prepared according to the procedure reported by Chen, *et al.*[65] Compound **50** was used to prepare the ethyl ester of *allo*-coronamic acid (**28**) according to the procedure reported by Groth, *et al.*[47] Tetrapeptide **25** was prepared according to the procedure reported by Bonaparte.[45]

3.1.2 Compounds

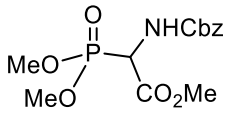

32

Methyl 2-benzyloxycarbonylamino-2-(dimethoxyphosphoryl)acetate 32. (CAF0083). A mixture of benzyl carbamate (1.19 g, 7.86 mmol), **37** (0.90 g, 10.22 mmol), and acetyl chloride (1.95 g, 24.80 mmol) in toluene (135 mL, 0.1M) was stirred at 60 °C for 14 h. The temperature was then increased to 75 °C, and trimethyl phosphite (2.44 g, 19.69 mmol) was added dropwise. The reaction was stirred for 3 h. The mixture was concentrated under reduced pressure, and the residue was dissolved in EtOAc (25 mL) and washed with a saturated solution of $NaHCO_3$ (25 mL). The organic layer was dried

($MgSO_4$), filtered, and concentrated to provide **32** as a light yellow solid. (1.56 g, 60% yield). ^1H and ^{13}C NMR data were consistent with the reported literature values.[31]

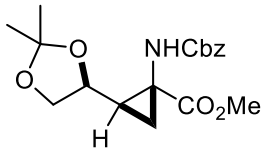

41

Methyl (1S,2R)-1-(((benzyloxy)carbonyl)amino)-2-((S)-2,2-dimethyl-1,3-dioxolan-4-yl)cyclopropane-1-carboxylate 41. (CAF0083). Compound **40** (0.74 g, 2.21 mmol) was stirred in DCM (22 mL, 0.1M) at -10 °C. Neat Et_2Zn (1.37 g, 11.06 mmol) was added dropwise to the solution, and diiodomethane (2.96 g, 11.06 mmol) was added immediately. The solution was warmed to room temperature over 3 h and then stirred an additional 3 h. The reaction was cooled to 0 °C and was quenched by the addition of a saturated solution of NH_4Cl (6 mL). The mixture was diluted with ether (10 mL), and a small amount of 0.1 M HCl (aq) (0.5 mL) was added. The layers were separated, then the organic layer was sequentially washed with saturated Na_2SO_3 (10 mL), saturated $NaHCO_3$ (10 mL), and brine (10 mL). The organic layer was dried ($MgSO_4$) and then concentrated under reduced pressure. The crude yield of 0.77 g (99% mass conversion) was sufficiently pure to use in the next step. ^1H and ^{13}C NMR data were consistent with the reported literature values.[24]

General procedure for peptide coupling. Preparation of 55, 57, 60.

A solution of *N*-Methylmorpholine (NMM) (0.307 g, 0.33 mL, 3.03 mmol), *N*-protected amino acid (0.708 mmol), EDCI•HCl (0.194 g, 1.011 mmol), and OxymaPure

(0.144 g, 1.011 mmol) was stirred in DMF (11.2 mL) at room temperature for 30 min. A solution of the *C*-protected amino acid (0.674 mmol) in DMF (7.5 mL) was added in one portion, and the mixture was stirred for 15 h. The mixture was concentrated under vacuum. Saturated $NaHCO_3$ (aq) (30 mL) was added then the aqueous phase was extracted with DCM (3 x 20 mL). The combined organic layers were washed with saturated $NaHCO_3$ (1 x 20 mL), 1 M HCl (3 x 20 mL), brine (1 x 30 mL), dried ($MgSO_4$), and concentrated under reduced pressure. The crude product was purified by flash column chromatography.

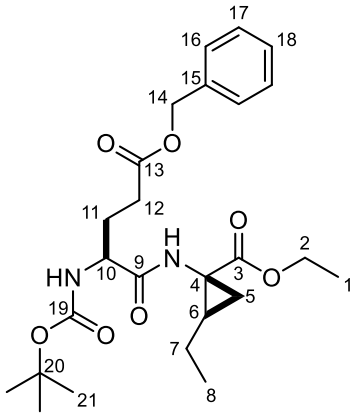

55

Ethyl (1S,2R)-1-((S)-5-(benzyloxy)-2-((tert-butoxycarbonyl)amino)-5-oxopentanamido)-2-ethylcyclopropane-1-carboxylate 55. (CAF0280). Prepared according to the general procedure. The crude material was purified by flash chromatography eluting with hexanes:EtOAc (2:1) to provide 71 mg (51%) as a white solid. ^{1}H NMR (400 MHz, $CDCl_3$) δ 7.37-7.29 (comp, 5 H), 6.69 (br. s, 1 H), 5.29 (m, 1H), 5.14 (s, 2 H), 4.20 (m, 1 H), 4.10 (q, *J* = 7.1 Hz, 2 H), 2.61 (comp, 2 H), 2.18 (m, 1 H), 1.95 (m, 1 H), 1.76-1.51 (comp, 4 H), 1.42 (s, 9 H), 1.19 (t, *J* = 7.1 Hz, 3 H, C1-H),

1.02 (t, J = 7.3 Hz, 3 H) 0.84 (comp, 1 H); ^{13}C NMR (400 MHz, $CDCl_3$) δ 173.4, 172.8, 172.2, 135.7, 128.6, 128.2, 66.6, 61.3, 37.5, 30.4, 29.8, 28.3, 28.1, 22.9, 21.7, 14.1, 13.4; Mass spectrum (ESI+) m/z = 499.2429 [$C_{25}H_{36}N_2O_7$ (M + Na) requires 499.2415].

NMR Assignments: ^{1}H NMR (400 MHz, $CDCl_3$) δ 7.37-7.29 (comp, 5 H, CAr-H), 6.69 (br. s, 1 H, amide N-H), 5.29 (m, 1H, carbamate N-H), 5.14 (s, 2 H, C14-H), 4.20 (m, 1 H, C10-H), 4.10 (q, J = 7.1 Hz, 2 H, C2-H), 2.61 (comp, 2 H, C12-H), 2.18 (m, 1 H, C11-H), 1.95 (m, 1 H, C11-H), 1.76-1.51 (comp, 4 H, C5-H and C7-H), 1.42 (s, 9 H, C21-H), 1.19 (t, J = 7.1 Hz, 3 H, C1-H), 1.02 (t, J = 7.3 Hz, 3 H, C8-H) 0.84 (m, 1 H, C6-H); ^{13}C NMR (400 MHz, $CDCl_3$) δ 173.4 (C3 or C9 or C13), 172.8 (C3 or C9 or C13), 172.2 (C3 or C9 or C13), 135.7 (C15), 128.6 (CAr), 128.2 (CAr), 66.6 (C14), 61.3 (C10), 37.5 (C2), 30.4 (C12), 29.8 (C6), 28.3 (C21), 28.1 (C5), 22.9 (C11), 21.7 (C7), 14.1 (C1), 13.4 (C8).

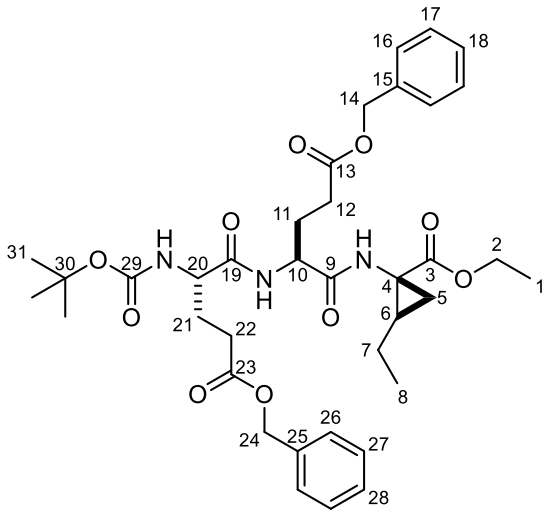

57

Ethyl (1S,2R)-1-((S)-5-(benzyloxy)-2-((S)-5-(benzyloxy)-2-((tert-butoxycarbonyl)amino)-5-oxopentanamido)-5-oxopentanamido)-2-ethylcyclopropane-1-carboxylate 57. (CAF0300). Prepared according to the general procedure. The crude material was purified by flash chromatography eluting with hexanes:EtOAc (1:1) to provide 108 mg (61%) as a white solid. ^{1}H NMR (400 MHz, $CDCl_3$) δ 7.39-7.30 (comp, 10 H), 5.20-5.07 (comp, 4 H), 4.47 (m, 1 H), 4.07 (comp, 3 H), 2.75-2.41 (comp, 4 H), 2.22-1.84 (comp, 4 H), 1.82-1.52 (comp, 4 H), 1.42, (s, 9 H), 1.17 (t, *J* = 7.1 Hz, 3 H), 1.01 (t, *J* = 7.3 Hz, 3 H), 0.89 (m, 1 H); ^{13}C NMR (400 MHz, $CDCl_3$) δ 174.3, 173.2, 172.2, 172.0, 171.6, 156.1, 135.6, 135.6, 128.6, 128.3, 128.3, 128.2, 80.6, 66.7, 66.7, 61.2, 55.0, 52.5, 37.7, 30.7, 30.4, 29.9, 28.3, 26.9, 22.3, 22.3, 21.5, 14.1, 13.5; Mass spectrum (ESI+) *m/z* = 696.3503 [$C_{37}H_{49}N_3O_{10}$ (M + H) requires 696.3491].

NMR Assignments: ^{1}H NMR (400 MHz, $CDCl_3$) δ 7.39-7.30 (comp, 10 H, CAr-H), 5.20-5.07 (comp, 4 H, C14-H, C24-H), 4.47 (m, 1 H, C10-H), 4.07 (comp, 3 H, C2-H,

C20-H), 2.75-2.41 (comp, 4 H, C12-H, C22-H), 2.22-1.84 (comp, 4 H, C11-H, C21-H), 1.82-1.52 (comp, 4 H, C5-H and C7-H), 1.42, (s, 9 H, C31-H), 1.17 (t, J = 7.1 Hz, 3 H, C1-H), 1.01 (t, J = 7.3 Hz, 3 H, C8-H) 0.89 (m, 1 H, C6-H); ^{13}C NMR (400 MHz, $CDCl_3$) δ 174.3 (C3 or C9 or C13 or C19 or C23), 173.2 (C3 or C9 or C13 or C19 or C23), 172.2 (C3 or C9 or C13 or C19 or C23), 172.0 (C3 or C9 or C13 or C19 or C23), 171.6 (C3 or C9 or C13 or C19 or C23), 156.1 (C29), 135.6 (C15 or C25), 135.6 (C15 or C25), 128.6 (CAr), 128.3 (CAr), 128.3 (CAr), 128.2 (CAr), 80.6 (C30), 66.7 (C14 or C24), 66.7 (C14 or C24), 61.2 (C10), 55.0 (C20), 52.5 (C4), 37.7 (C2), 30.7 (C12 or C22), 30.4 (C12 or C22), 29.9 (C6), 28.3 (C31), 26.9 (C5), 22.36 (C11 or C21), 22.3 (C11 or C21), 21.5 (C7), 14.1 (C1), 13.5 (C8).

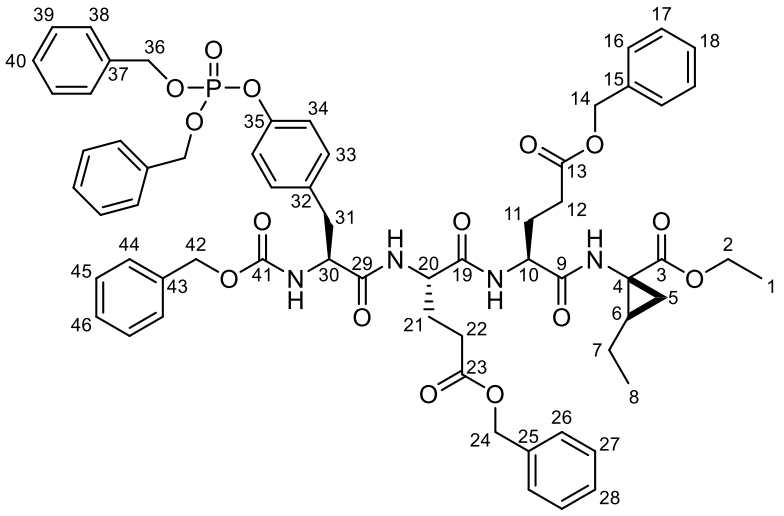

Ethyl (1S,2R)-1-((5S,8S,11S)-8,11-bis(3-(benzyloxy)-3-oxopropyl)-5-(4-((bis(benzyloxy)phosphoryl)oxy)benzyl)-3,6,9-trioxo-1-phenyl-2-oxa-4,7,10-triazadodecan-12-amido)-2-ethylcyclopropane-1-carboxylate 60. (CAF1023). Prepared according to the general procedure. The crude material was purified by flash chromatography eluting with hexanes:EtOAc (1:2) to provide 69 mg (55%) as a white solid. ^{1}H NMR (400 MHz, $CDCl_3$) δ 7.35-7.28 (comp, 20 H), 7.25 (comp, 2 H), 7.05 (comp, 2 H), 5.12-5.00 (comp, 4 H), 4.46-4.25 (comp, 3 H), 4.10 (q, *J* = 7.1 Hz, 2 H), 3.06 (m, 1 H), 2.88 (m, 1 H), 2.68-2.32 (comp, 4 H), 2.29-1.87 (comp, 4 H), 1.79-1.51 (comp, 4 H), 1.15 (t, *J* = 7.1 Hz, 3 H), 1.00 (t, *J* = 7.3 Hz, 3 H) 0.87 (m, 1 H); ^{13}C NMR (400 MHz, $CDCl_3$) δ 174.1, 173.5, 172.3, 172.2, 171.8, 170.6, 156.5, 135.8, 135.7, 135.4, 135.3, 130.4, 128.6, 128.5, 128.5, 128.4, 128.3, 128.2, 128.2, 128.2, 128.1, 128.00, 127.95, 120.4, 70.0, 67.4, 66.8, 66.5, 61.2, 56.6, 52.9, 37.7, 30.7, 30.6, 30.0, 26.9, 26.3, 22.4, 22.4, 21.6, 14.1, 13.6; Mass spectrum (ESI+) *m*/*z* = 1175.4401 [$C_{63}H_{69}N_4O_{15}$ (M + Na) requires 1175.4389].

NMR Assignments: ^{1}H NMR (400 MHz, $CDCl_3$) δ 7.35-7.28 (comp, 20 H, CAr-H), 7.25 (comp, 2 H, C33-H or C34-H), 7.05 (comp, 2 H, C33-H or C34-H), 5.12-5.00 (comp, 4 H, C14-H, C24-H, C36-H, C42-H), 4.46-4.25 (comp, 3 H, C10-H, C20-H, C30-H), 4.10 (q, *J* = 7.1 Hz, 2 H, C2-H), 3.06 (m, 1 H, C31-H), 2.88 (m, 1 H, C31-H), 2.68-2.32 (comp, 4 H, C12-H, C22-H), 2.29-1.87 (comp, 4 H, C11-H, C21-H), 1.79-1.51 (comp, 4 H, C5-H and C7-H), 1.15 (t, *J* = 7.1 Hz, 3 H, C1-H), 1.00 (t, *J* = 7.3 Hz, 3 H, C8-H) 0.87 (m, 1 H, C6-H); ^{13}C NMR (400 MHz, $CDCl_3$) δ 174.1 (C3 or C9 or C13 or C19 or C23 or C29), 173.5 (C3 or C9 or C13 or C19 or C23 or C29), 172.3 (C3 or C9 or C13 or C19 or C23 or C29), 172.2 (C3 or C9 or C13 or C19 or C23 or C29), 171.8 (C3 or C9 or C13 or C19 or C23 or C29), 170.6 (C3 or C9 or C13 or C19 or C23 or C29), 156.5 (C46), 135.75 (C15 or C25 or C42 or C37), 135.7 (C15 or C25 or C42 or C37), 135.4, (C15 or C25 or C42 or C37), 135.3 (C15 or C25 or C42 or C37), 130.4 (C32), 128.6 (CAr), 128.5 (CAr), 128.5 (CAr), 128.4 (CAr), 128.3 (CAr), 128.2 (CAr), 128.2 (CAr), 128.2 (CAr), 128.1 (CAr), 128.00 (CAr), 127.95 (CAr), 120.4 (C35), 70.0 (C30), 67.4 (C14 or C24 or C41 or C36), 66.8 (C14 or C24 or C41 or C36), 66.5 (C14 or C24 or C41 or C36), 61.2 (C10), 56.6 (C20), 52.9 (C4), 37.7 (C2), 30.7 (C12 or C22), 30.6 (C12 or C22), 30.0 (C6), 26.9 (C5), 26.3 (C31), 22.4 (C11 or C21), 22.4 (C11 or C21), 21.6 (C7), 14.1 (C1), 13.6 (C8).

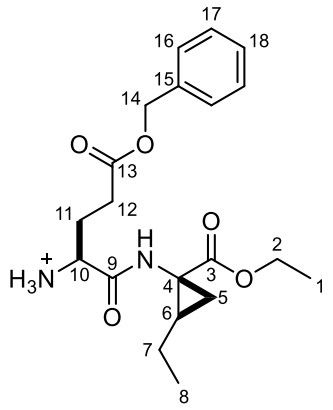

56

(S)-5-(Benzyloxy)-1-(((1S,2R)-1-(ethoxycarbonyl)-2-ethylcyclopropyl)amino)-1,5-dioxopentan-2-aminium trifluoroacetate 56. (CAF0304). Trifluoroacetic acid (TFA) (0.995 g, 0.65 mL, 8.729 mmol) was added to a solution of dipeptide **55** (0.104 g, 0.218 mmol) in DCM (2.2 mL) at room temperature and was stirred for 4 h. The solution was concentrated under reduced pressure, and then the residue was azeotroped with toluene (3 x 15 mL) to give 0.106 g (quant. yield) of crude **56** as a sticky yellow resin that was used without further purification. ^{1}H NMR (400 MHz, $CDCl_3$) δ 7.37-7.29 (comp, 5 H), 5.09 (comp, 2 H), 4.65 (br, 1 H), 4.06 (q, *J* = 7.1 Hz, 2 H), 2.53 (t, *J* = 7.4 Hz, 2 H), 2.09 (m, 1 H), 1.87 (m, 1 H), 1.70-1.52 (comp, 4 H, C5-H and C7-H), 1.19 (t, *J* = 7.1 Hz, 3 H, C1-H), 1.00 (t, *J* = 7.3 Hz, 3 H, C8-H) 0.85 (comp, 1 H, C6-H); Mass spectrum (ESI+) *m*/*z* = 377.2085 [$C_{20}H_{28}N_2O_5$ (M + H) requires 377.2071].

NMR Assignments: ^{1}H NMR (400 MHz, $CDCl_3$) δ 7.37-7.29 (comp, 5 H, CAr-H), 5.09 (comp, 2 H, C14-H), 4.65 (br, 1 H, C10-H), 4.06 (q, *J* = 7.1 Hz, 2 H, C2-H), 2.53 (t, *J* = 7.4 Hz, 2 H, C12-H), 2.09 (m, 1 H, C11-H), 1.87 (m, 1 H, C11-H), 1.70-1.52 (comp,

4 H, C5-H and C7-H), 1.19 (t, *J* = 7.1 Hz, 3 H, C1-H), 1.00 (t, *J* = 7. Hz, 3 H, C8-H) 0.85 (comp, 1 H, C6-H).

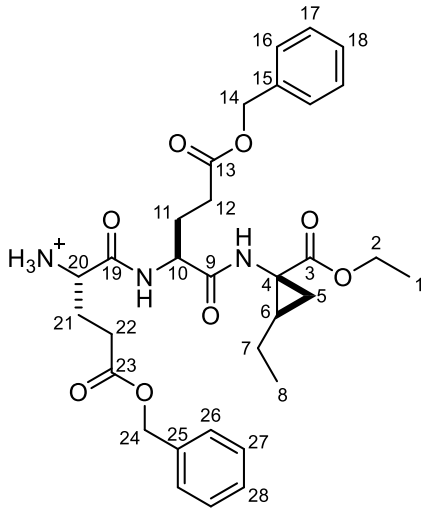

58

(S)-5-(Benzyloxy)-1-(((S)-5-(benzyloxy)-1-(((1S,2R)-1-(ethoxycarbonyl)-2-ethylcyclopropyl)amino)-1,5-dioxopentan-2-yl)amino)-1,5-dioxopentan-2-aminium trifluoroacetate 58. (CAF1022). TFA (0.56 g, 0.37 mL, 4.944 mmol) was added to a solution of tripeptide **57** (86 mg, 0.124 mmol) in DCM (1.3 mL) at room temperature and was stirred for 4 h. The solution was concentrated under reduced pressure, and then the residue was azeotroped with toluene (3 x 15 mL) to give 73 mg (quant. yield) of crude **58** as a yellow oil that was used without further purification. ^{1}H NMR (400 MHz, $CDCl_3$) δ 7.39-7.29 (comp, 10 H), 5.17-5.06 (comp, 4 H), 4.45 (m, 1 H), 4.09 (q, *J* = 7.1 Hz, 2 H), 3.38 (m, 1 H), 2.68-2.42 (comp, 4 H), 2.30-1.78 (comp, 4 H), 1.71-1.50 (comp, 4 H), 1.18 (t, *J* = 7.1 Hz, 3 H), 1.01 (t, *J* = 7.3 Hz, 3 H) 0.82 (m, 1 H; ^{13}C NMR (400 MHz, $CDCl_3$) δ 174.8, 173.3, 173.1, 172.4, 172.2, 135.7, 135.7, 128.6, 128.3, 66.6, 66.5, 61.3, 54.5, 51.8,

37.6, 30.7, 30.1, 29.7, 27.6, 22.8, 22.8, 21.7, 14.1, 13.5; Mass spectrum (ESI+) *m*/*z* = 618.2802 [$C_{32}H_{41}N_3O_8$ (M + Na) requires 618.2786].

NMR Assignments: ^{1}H NMR (400 MHz, $CDCl_3$) δ 7.39-7.29 (comp, 10 H, CAr-H), 5.17-5.06 (comp, 4 H, C14-H, C24-H), 4.45 (m, 1 H, C10-H), 4.09 (q, *J* = 7.1 Hz, 2 H, C2-H), 3.38 (m, 1 H, C20-H), 2.68-2.42 (comp, 4 H, C12-H, C22-H), 2.30-1.78 (comp, 4 H, C11-H, C21-H), 1.71-1.50 (comp, 4 H, C5-H and C7-H), 1.18 (t, *J* = 7.1 Hz, 3 H, C1-H), 1.01 (t, *J* = 7. Hz, 3 H, C8-H) 0.82 (m, 1 H, C6-H); ^{13}C NMR (400 MHz, $CDCl_3$) δ 174.8 (C3 or C9 or C13 or C19 or C23), 173.3 (C3 or C9 or C13 or C19 or C23), 173.1 (C3 or C9 or C13 or C19 or C23), 172.4 (C3 or C9 or C13 or C19 or C23), 172.2 (C3 or C9 or C13 or C19 or C23), 135.7 (C15 or C25), 135.7 (C15 or C25), 128.6 (CAr), 128.3 (CAr), 66.6 (C14 or C24), 66.5 (C14 or C24), 61.3 (C10), 54.5 (C20), 51.8 (C4), 37.6 (C2), 30.7 (C12 or C22), 30.1 (C12 or C22), 29.7 (C6), 27.6 (C5), 22.8 (C11 or C21), 22.8 (C11 or C21), 21.7 (C7), 14.1 (C1), 13.5 (C8).

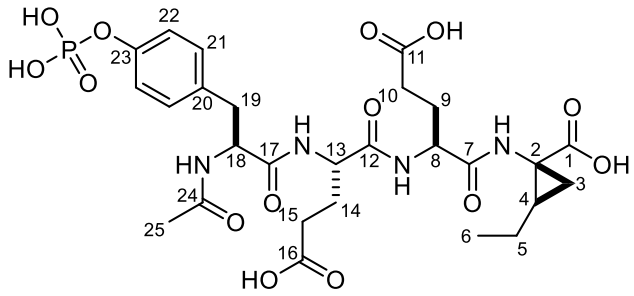

26

(1S,2R)-1-((S)-2-((S)-2-((S)-2-Acetamido-3-(4-(phosphonooxy)phenyl)propanamido)-4-carboxybutanamido)-4-carboxybutanamido)-2-ethylcyclopropane-1-carboxylic acid 26. (CAF1118). 10% Pd/C (3 mg, 10% wt) was added to a solution of tetrapeptide **60** (27 mg, 0.023 mmol) in MeOH/H_2O (12 mL, 5:1), and the flask was purged three times with H_2. The suspension was stirred under H_2 (1 atm) for 1.5 h at room temperature. The suspension was filtered through a pad of celite, and the pad was washed with MeOH (5 mL) and H_2O (10 mL). The filtrate was concentrated under reduced pressure. The residue was dissolved in THF/H_2O (5.2 mL, 0.5:4.7) and LiOH•H_2O was added (45 mg, 1.063 mmol) to the solution. The solution was stirred at room temperature for 24 h, then the reaction was concentrated under reduced pressure. The residue was dissolved in dioxane/H_2O (0.55 mL, 4:1) and Ac_2O (0.214 g, 0.20 mL, 2.10 mmol) was added. The solution was stirred at room temperature for 18 h, then MeOH (1 mL) was added. The reaction was concentrated under reduced pressure. The crude product was purified by RP HPLC with a gradient of 0-30% acetonitrile in H_2O over 30 min (12.8 min) and lyophilized to provide 2.2 mg (17%) of **26** a white solid. ^{1}H NMR (400 MHz, DMSO-d_6) δ 8.11 (m, 1 H), 8.05 (m, 1 H), 7.95 (m, 1 H), 7.88 (m, 1 H), 6.97 (comp, 4 H), 4.41 (app q, J = 6.8 Hz, 1 H), 4.20 (m, 1 H), 4.09 (m, 1 H), 2.86-2.73 (comp, 2 H), 2.24 (comp, 2 H), 2.05 (comp,

2H), 1.81 (s, 3 H), 1.78-1.64 (comp, 4 H), 1.51-1.43 (comp, 3 H), 1.29 (m, 1 H), 0.95-0.86 (comp, 4 H); ^{13}C NMR (400 MHz, DMSO-d_6) δ 174.9, 174.6, 174.5, 172.9, 172.8, 171.3, 170.1, 153.0, 130.4, 130.0, 120.0, 54.6, 52.74, 52.72, 52.5, 37.0, 30.9, 30.7, 29.4, 28.6, 27.7, 27.3, 22.9, 21.6, 14.1; Mass spectrum (ESI+) m/z = 695.1945 [$C_{27}H_{37}N_4O_{14}$ (M + Na) requires 695.1936].

NMR Assignments: ^{1}H NMR (400 MHz, DMSO-d_6) δ 8.11 (m, 1 H, N-H), 8.05 (m, 1 H, N-H), 7.95 (m, 1 H, N-H), 7.88 (m, 1 HN-H), 6.97 (comp, 4 H, C21-H and C22-H), 4.41 (app q, J = 6.8 Hz, 1 H, C18-H), 4.20 (m, 1 H, C8-H), 4.09 (m, 1 H, C13-H), 2.86-2.73 (comp, 2 H, C19-H), 2.24 (comp, 2 H, C10-H or C-15 H), 2.05 (comp, 2H, C10-H or C15-H), 1.81 (s, 3 H, C25-H), 1.78-1.64 (comp, 4 H, C9-H and C14-H), 1.51-1.43 (comp, 3 H, C4-H and C5-H), 1.29 (m, 1 H, C3-H), 0.95-0.86 (comp, 4 H, C3-H and C6-H); ^{13}C NMR (400 MHz, DMSO-d_6) δ 174.9 (C1 or C11 or C16), 174.6 (C1 or C11 or C16), 174.5 (C1 or C11 or C16), 172.9 (C7 or C12 or C17 or C24), 172.8 (C7 or C12 or C17 or C24), 171.3 (C7 or C12 or C17 or C24), 170.1 (C7 or C12 or C17 or C24), 153.0 (C23), 130.4 (C21), 130.0 (C22), 120.0 (C20), 54.6 (C18), 52.7 (C8 or C13), 52.7 (C8 or C13), 52.5 (C2), 37.0 (C19), 30.9 (C10 or C15), 30.7 (C10 or C15), 29.4 (C4), 28.6 (C3), 27.7 (C9 or 14), 27.3 (C9 or 14), 22.9 (C25), 21.6 (C5), 14.1 (C6).

3.2 BIOLOGICAL MATERIALS AND METHODS

3.2.1 Preparation of Src SH2

A 30 mL culture of LB/amp (100 μg/mL) was inoculated with a single colony of *E. coli* bearing the Src SH2 domain plasmid overnight at 37 °C in a shaker at 225 rpm. The culture was used to inoculate a larger culture (1 L) of LB/amp (100 μg/mL) which was incubated at 30 °C in a shaker at 75 rpm until an OD_{600} value of 0.8-1.0 was reached. Expression of protein was induced by adding IPTG (0.1 mM final concentration) and the cultures continued to incubate at 30 °C for an additional 15-16 h. The cultures were centrifuged at 8,000xg at 4 °C for 15 min. The supernatant was decanted and the cell pellets were stored at -80 °C until they were to be lysed.

One pellet was resuspended in 30 mL lysis buffer (20 mM sodium citrate, 1 mM EDTA, 0.1 mM PMSF, 0.1% v/v β-mercaptoethanol (BME), pH = 6.0 ± 0.05). The cells were lysed by probe sonication on ice for 2 min (2 sec pulse, 8 sec rest) and then centrifuged at 10,000xg at 4 °C for 45 min. The supernatant was reserved and the pellet was discarded

The supernatant (~35 mL) was loaded onto a 15 mL SP-sepharose ion exchange column equilibrated with Buffer A (20 mM sodium citrate, 1 mM EDTA, 0.1% v/v β-mercaptoethanol (BME), pH = 6.0 ± 0.05) (3 mL/min). The lysate was eluted with Buffer A (75 mL), then eluted with a gradient of Buffer A and Buffer B (20 mM sodium citrate, 1 mM EDTA, 0.1% v/v β-mercaptoethanol (BME), pH = 6.0 ± 0.05) (0%-50% Buffer B over 100 mL). The column was washed with 100% Buffer B (75 mL), and then washed with Buffer A (75 mL). The fractions containing Src SH2 were concentrated to a volume of ~0.7-1.0 mL.

The concentrate from the previous step was loaded onto a 100 mL Size Exclusion column and eluted with Buffer C (20 mM MES, 5 mM DTT, 1 mM EDTA, 50 mM NaCl

20 mM sodium citrate, 1 mM EDTA, 0.1% v/v β-mercaptoethanol (BME), pH = 6.0 ± 0.05) (0.5 mL/min). The fractions containing Src SH2 were dialyzed using 1000-3000 MW cutoff dialysis tubing in HEPES buffer (20 mM HEPES, 1 mM EDTA, 100 mM NaCl, 1 mM BME, pH = 7.3 ± 0.05) (2 L) for 24 h. The dialysis buffer was replaced with a fresh solution of the same HEPES buffer and the protein solution was dialyzed for 24 h. Protein concentration was determined by using UV-Vis spectroscopy using the extinction coefficient for the Src SH2 domain (ε_{280} = 14,700 $M^{-1}cm^{-1}$).[35] Concentrations of 60-80 μM were acceptable for ITC experiments.

3.2.2 Isothermal Titration Calorimetry

Ligand solutions were prepared to 15x concentration of protein by weighing the solids on an analytical balance and then dissolving in 996 μL HEPES buffer. NaOH (aq) was added to adjust the pH to 7.3 ± 0.05. The ligand and protein solutions were filtered through a 0.2 μm sterile filter and degassed for 15 min prior to the ITC experiment.

Plots were obtained for the titration of Src SH2 domain with the indicated ligands in HEPES buffer at 25 °C. Titration data was obtained from 1 x 2 μL and 39 x 8 μL injections of ligand, resulting in peaks corresponding to the heats of complexation (μcal/s).

Integrated ITC data provides the heat of binding per mol of injected ligand. The data were corrected by subtracting the heat of addition of the final injection, at which point all protein is complexed and the injection represents a blank titration. The trace was determined by applying a nonlinear least squares fit to determine binding stoichiometry n, K_a, and $\Delta H°$. The values for $\Delta G°$ and $\Delta S°$ were calculated from K_a and $\Delta H°$. Raw values of $0.9 < n < 1.2$ were considered acceptable, and n was corrected to 1.000 for the reported data.

1 (pYEEI)

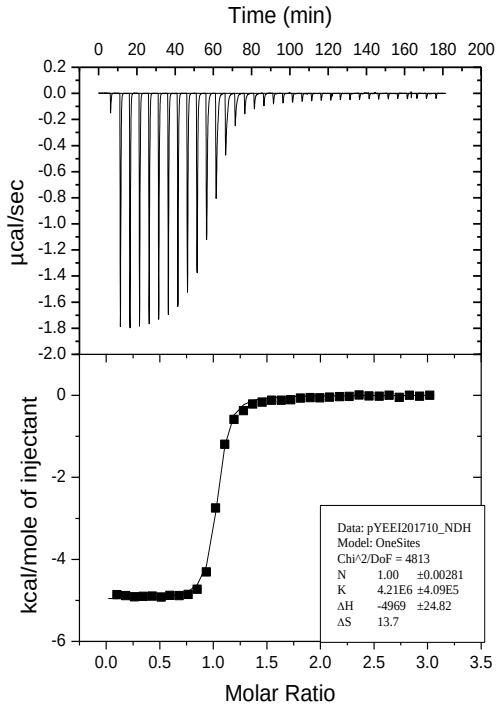

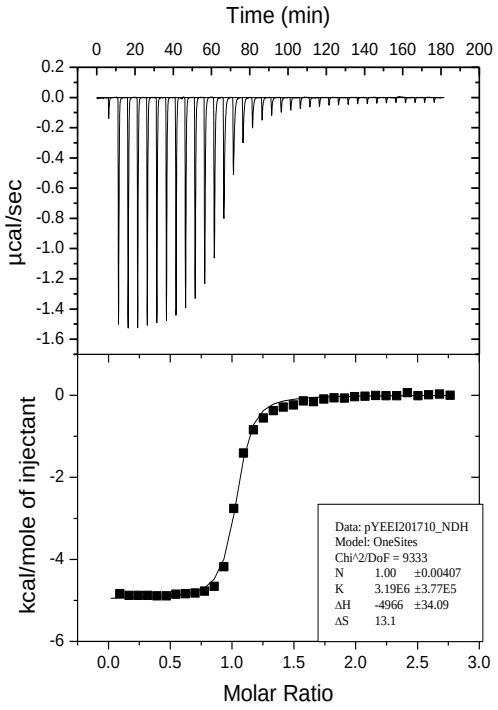

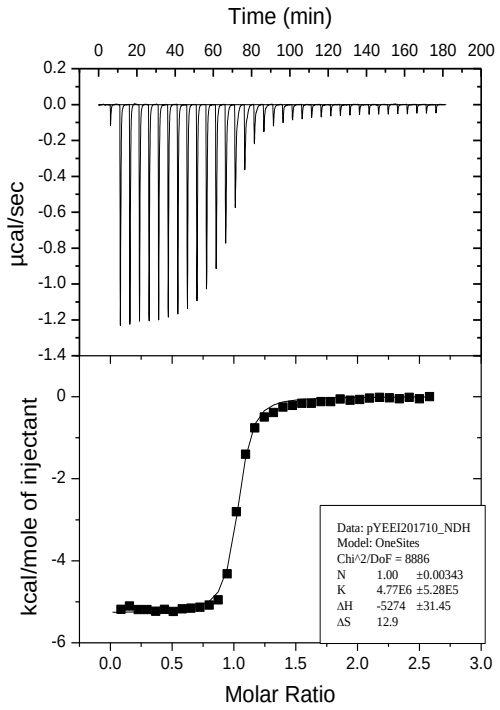

Average (from 3 titrations)

$K_a = 4.2\ (\pm\ 0.3)\ 10^6\ M^{-1}$
$\Delta G° = -9.03 \pm 0.05$ kcal/mol
$\Delta H° = -5.15 \pm 0.25$ kcal/mol
$T\Delta S° = -3.89 \pm 0.64$ kcal/mol

26 (pYEEcP)

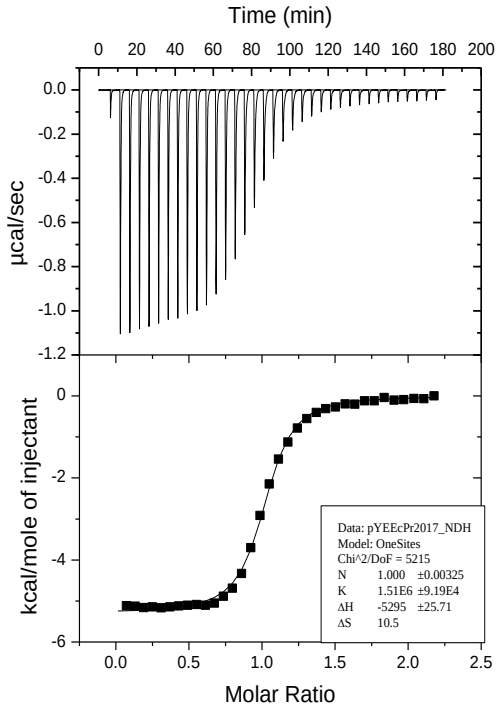

One experiment

K_a = 1.5 x 10^6 M^{-1}
$\Delta G°$ = -8.43 kcal/mol
$\Delta H°$ = -5.30 kcal/mol
$T\Delta S°$ = -3.13 kcal/mol

27 (pYEEnV)

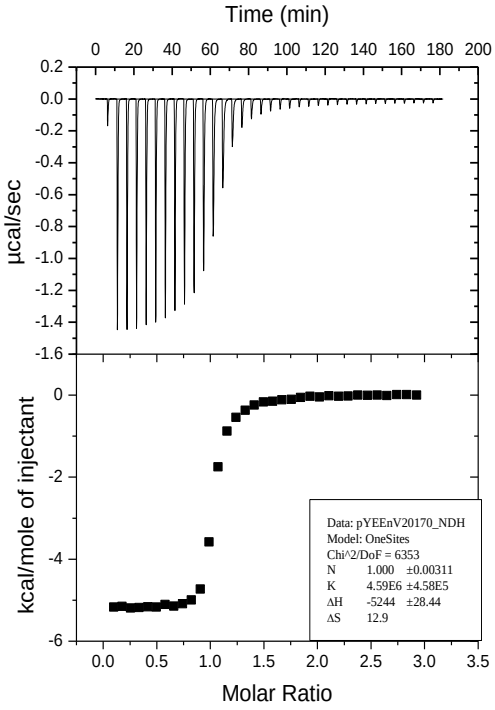
Time (min)
µcal/sec
kcal/mole of injectant
Molar Ratio
Data: pYEEnV20170_NDH
Model: OneSites
Chi^2/DoF = 6353
N 1.000 ±0.00311
K 4.59E6 ±4.58E5
ΔH -5244 ±28.44
ΔS 12.9

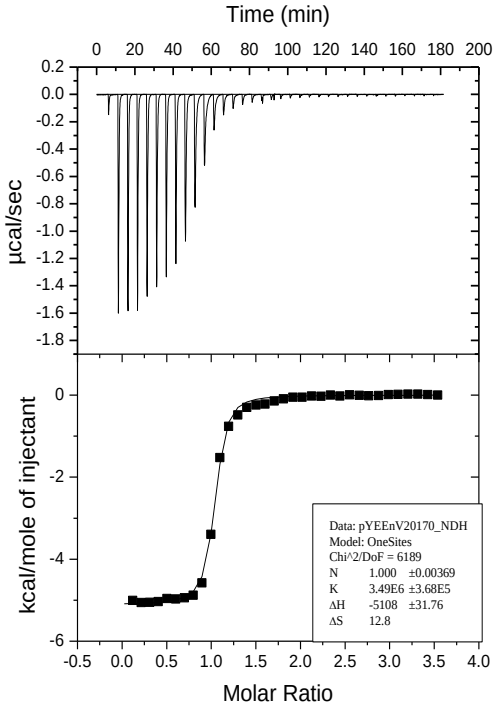
Time (min)
µcal/sec
kcal/mole of injectant
Molar Ratio
Data: pYEEnV20170_NDH
Model: OneSites
Chi^2/DoF = 6189
N 1.000 ±0.00369
K 3.49E6 ±3.68E5
ΔH -5108 ±31.76
ΔS 12.8

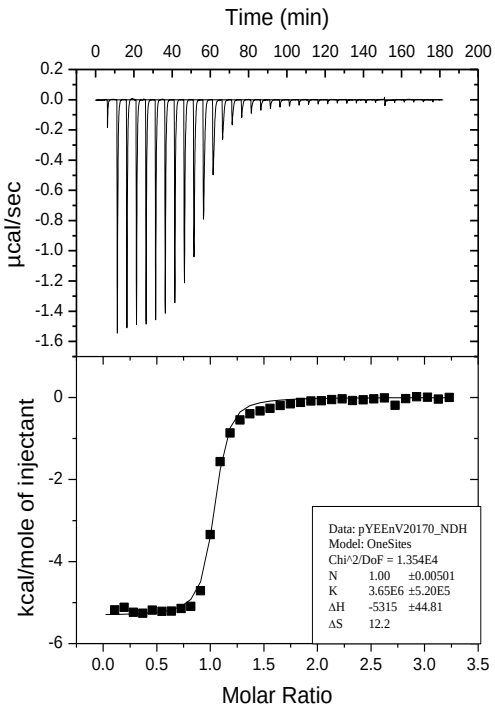
Time (min)
µcal/sec
kcal/mole of injectant
Molar Ratio
Data: pYEEnV20170_NDH
Model: OneSites
Chi^2/DoF = 1.354E4
N 1.00 ±0.00501
K 3.65E6 ±5.20E5
ΔH -5315 ±44.81
ΔS 12.2

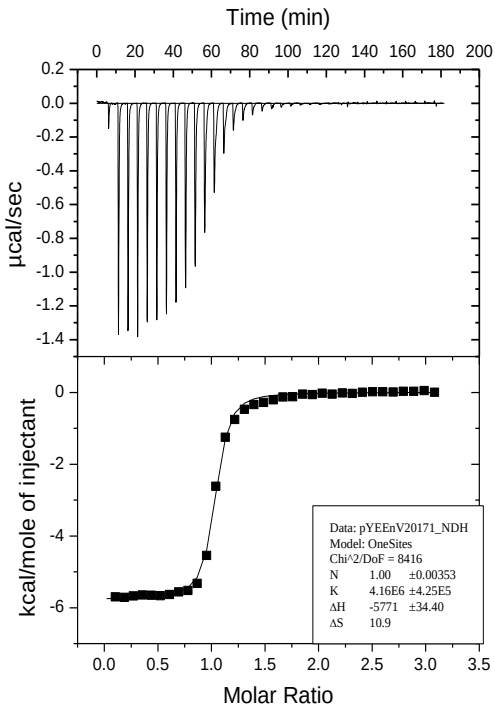
Time (min)
µcal/sec
kcal/mole of injectant
Molar Ratio
Data: pYEEnV20171_NDH
Model: OneSites
Chi^2/DoF = 8416
N 1.00 ±0.00353
K 4.16E6 ±4.25E5
ΔH -5771 ±34.40
ΔS 10.9

Average (from 4 titrations)

K_a = 4.0 (± 0.3) 10^6 M^{-1}
$\Delta G°$ -9.00 ± 0.05 kcal/mol
$\Delta H°$ = -5.36 ± 0.34 kcal/mol
$\Delta S°$ = -3.64 ± 0.66 kcal/mol

References

(1) Martin, S. F.; Clements, J.H. "Correlating Structure and Energetics in Protein-Ligand Interactions: Paradigms and Paradoxes." *Annu. Rev. Biochem* **2013**, *82*, 267-263.

(2) Warren, G. L.; Andrews, C.W.; Capelli, A.M.; Clarke, B.; LaLonde, J.; Lambert, M.H.; Lindvall, M.; Nevins, N.; Semus, S.F.; Senger, S.; Tedesco, G.; Wall, I.D.; Woolven, J. M.; Peishoff, C.E.; Head, M.S. "A Critical Assessment of Docking Programs and Scoring Functions." *J. Med. Chem.* **2006**, *49*, 5912-5931.

(3) Mobley, D. L.; Dill, K. A. "Binding of Small-Molecule Ligands to Proteins: "What You See" Is Not Always "What You Get."" *Structure* **2009**, *17*, 489–498.

(4) Gohlke, H.; Klebe, G. "Approaches to the Description and Prediction of the Binding Affinity of Small-Molecule Ligands to Macromolecular Receptors." *Angew. Chemie Int. Ed.* **2002**, *41*, 2644–2676.

(5) Babine, R.E.; Bender, S.L. "Molecular Recognition of Protein-Ligand Complexes: Applications to Drug Design." *Chem. Rev.* **1997**, *97*, 1359-1472.

(6) Reichelt, A.; Martin, S. F. "Synthesis and Properties of Peptidomimetics: Design Rationale for Cyclopropane-Derived Peptidomimetics." *Acc. Chem Res.* **2006**, *39*, 433-442.

(7) Whitesides, G. M.; Krishnamurthy, V. M. "Designing Ligands to Bind Proteins." *Quart. Rev. Biophys.* **2006**, *38*, 385.

(8) Williams, M.A.; Ladbury, J.E. "Hydrogen Bonds in Protein-Ligand Complexes". *Protein-Ligand Interactions: From Molecular Recognition to Drug Design*; Bohm, H.J.; Schneider, G., Eds.; Wiley-VCH Verlag GmbH &Co. KGaA, Weinheim, FRG, 2003.

(9) Chang, C.E.A.; Chen, W.; Gilson, M.K. "Ligand Configurational Entropy and Protein Binding." *Proc. Nat. Acad. Sci. USA* **2007**, *104*, 1534-1539.

(10) Perola, E.; Charifson, P.S. "Conformational Analysis of Drug-Like Molecules Bound to Proteins: An Extensive Study of Ligand Reorganization Upon Binding." *J. Med. Chem.* **2004**, *47*, 2499-2510.

(11) Bursavich, M. G.; Rich, D. H. "Designing Non-Peptide Peptidomimetics in the 21st Century: Inhibitors Targeting Conformational Ensembles." *J. Med. Chem.* **2002**, *45*, 541-558.

(12) Hanessian, S.; McNaughton-Smith, G.; Lombart, H.-G.; Lubell, W. D. "Design and Synthesis of Conformationally Constrained Amino Acids as Versatile Scaffolds and Peptide Mimetics." *Tetrahedron* **1997**, *53*, 12789-12854.

(13) Khan, A.R.; Parrish, J.C.; Fraser, M.E.; Smith, W.W.; Bartlett, P.A.; James, M.N.G. "Lowering the Entropic Barrier for Binding Conformationally Flexible Inhibitors to Enzymes." *Biochemistry* **1998**, *37*, 16839-16845.

(14) Benfield, A.P.; Teresk, M.G.; Plake, H.R.; Delorbe, J.E.; Millspaugh, L.E.; Martin, S.F. "Ligand Preorganization May Be Accompanied by Entropic Penalties in Protein-Ligand Interactions." *Angew. Chem. Int. Ed.* **2006**, *45*, 6830-6835.

(15) Meyer, J. H.; Bartlett, P. A. "Macrocyclic Inhibitors of Penicillopepsin. 1. Design, Synthesis, and Evaluation of an Inhibitor Bridged Between P2 and P1." *J. Am. Chem. Soc.* **1998**, *120*, 4600-4609.

(16) Gerhard, U.; Searle, M. S.; Williams, D. H. "The Free Energy Change of Restricting a Bond Rotation in the Binding of Peptide Analogues to Vancomycin Group Antibiotics." *Bioorg. Med. Chem. Lett.* **1993**, *3*, 803-808.

(17) Chandler, D. "Interfaces and the Driving Force of Hydrophobic Assembly." *Nature* **2005**, *437*, 640-647.

(18) Carey, C.; Cheng, Y.K.; Rossky, P.J. "Hydration Structure of the A-Chymotrypsin Substrate Binding Pocket: The Impact of Constrained Geometry." *Chem. Phys.* **2000**, *258*, 415-425.

(19) Lee, C.Y.; McCammon, J.A.; Rossky, P.J. “The Structure of Liquid Water at an Extended Hydrophobic Surface.” *J. Chem. Phys.* **1984**, *80*, 4448.

(20) Myslinski, J.M.; Delorbe, J.E.; Clements, J.H.; Martin, S.F. “Protein-Ligand Interactions: Thermodynamic Effects Associated with Increasing Nonpolar Surface Area.” *J. Am. Chem. Soc.***2011**, *133*, 18518-18521.

(21) Chondera, J.D.; Mobley, D.L. “Entropy-Enthalpy Compensation: Role and Ramifications in Biomolecular Ligand Recognition and Design.” *Annu. Rev. Biophys.* **2013**, *42*, 121-141.

(22) Gilli, P.; Ferretti, V.; Gilli, G.; Borea, P. A. “Enthalpy-Entropy Compensation in Drug-Receptor Binding.” *J. Phys. Chem.* **1994**, *98*, 1515-1518.

(23) Dunitz, J. D. “Win Some, Lose Some: Enthalpy-Entropy Compensation in Weak Intermolecular Interactions.” *Chem. Biol.* **1995**, *2*, 709-712.

(24) Sharp, K. “Entropy-Enthalpy Compensation: Fact or Artifact?” *Protein Science*, **2001**, *10*, 661-667.

(25) Ford, D.M. “Enthalpy-Entropy Compensation Is Not a General Feature of Weak Association.” *J. Am. Chem. Soc.* **2005**, *127*, 16167-16170.

(26) Lafont, V.; Armstrong, A. A.; Ohtaka, H.; Kiso, Y.; Mario-Amzel, L.; Freire, E. “Compensating Enthalpic and Entropic Changes Hinder Binding Affinity Optimization.” *Chem. Biol. Drug Des.* **2007**, *69*, 413-422.

(27) Wiseman, T.; Williston, S.; Brandts, J.F.; Lin, L.N. “Rapid Measurement of Binding Constants and Heats of Binding Using a New Titration Calorimeter.” *Anal. Biochem*. **1989**, *179*, 131-137.

(28) Velazquez-Campoy, A.; Freire, E. “Isothermal Titration Calorimetry to Determine Association Constants for High-Affinity Ligands.” *Nat. Protocols* **2006**, *1*, 186-191.

(29) Hruby, V. J.; Li, G.; Haskell-Luevano, C.; Shenderovich, M. “Design of Peptides, Proteins, and Peptidomimetics in Chi Space.” *Biopolymers* **1997**, *43*, 219-266.

(30) Avan, I.; Hall, C. D.; Katritzky, A. R. “Peptidomimetics via Modifications of Amino Acids and Peptide Bonds.” *Chem. Soc. Rev.* **2014**, *43*, 3575-3594.

(31) Shakespeare, W.; Yang, M.; Bohacek, R.; Cerasoli, F.; Stebbins, K.; Sundaramoorthi, R.; Asimioara, M.; Vu, C.; Pradeepan, S.; Metcalf, C.; Haraldson, C.; Merry, T.; Dalgarno, D.; Narula, S.; Hatada, M.; Lu, X.; van Schravendijk, M. R.; Adams, S.; Violette, S.; Smith, J.; Guan, W.; Bartlett, C.; Herson, J.; Iuliucci, J.; Weigele, M.; Sawyer, T. “Structure-Based Design of an Osteoclast-Selective Nonpeptide Src Homology 2 Inhibitor with *in vivo* Antiresorptive Activity.” *Proc. Natl. Acad. Sci. U.S.A.* **2000**, *97*, 9373-9378.

(32) Machida, K.; Mayer, B. J. “The SH2 Domain: Versatile Signaling Module and Pharmaceutical Target.” *Biochim. Et Biophys. Acta* **2005**, 1-25.

(33) Waksman, G.; Shoelson, S.E.; Pant, N.; Cosburn, D.; Kuriyan, J. “Binding of a High Affinity Phosphotyrosyl Peptide to the Src SH2 Domain: Crystal Structures of the Complexed and Peptide-Free Forms.” *Cell* **1993**, *72*, 779-790.

(34) Bradshaw, J. M.; Grucza, R. A.; Ladbury, J. E.; Waksman, G. “Probing the ‘Two-Pronged Plug Two-Holed Socket’ Model for the Mechanism of Binding of the Src SH2 Domain to Phosphotyrosyl Peptides: A Thermodynamic Study.” *Biochemistry* **1998**, *37*, 9083-9090.

(35) Bradshaw, J. M.; Mitaxov, V.; Waksman, G. “Investigation of Phosphotyrosine Recognition by the SH2 Domain of the Src Kinase.” *J. Mol. Biol.* **1999**, *293*, 971-985.

(36) Bradshaw, J. M.; Waksman, G. “Calorimetric Examination of High-Affinity Src SH2 Domain-Tyrosyl Phosphopeptide Binding: Dissection of the Phosphopeptide Sequence Specificity and Coupling Energetics.” *Biochemistry* **1999**, *38*, 5147-5154.

(37) Davidson, J. P.; Lubman, O.; Rose, T.; Waksman, G.; Martin, S. F. "Calorimetric and Structural Studies of 1,2,3-Trisubstituted Cyclopropanes as Conformationally Constrained Peptide Inhibitors of Src SH2 Domain Binding." *J. Am. Chem. Soc.* **2002**, *124*, 205-215.

(38) Gravenstreter, A. N. "Design and Synthesis of Conformationally Constrained Src SH2 Ligands for Protein-Ligand Thermodynamic Evaluation." University of Texas at Austin, 2016.

(39) Ward, J.M.; Gorenstein, N.M.; Tian, J.; Martin, S.F.; Post, C.B. "Constraining Binding Hot Spots: NMR and Molecular Dynamics Simulations Provide a Structural Explanation for Enthalpy-Entropy Compensation in SH2-Ligand Binding." *J. Am. Chem. Soc.* **2010**, *132*, 11058-11070.

(40) Harris, T. K.; Mildvan, A. S. "High-Precision Measurement of Hydrogen Bond Lengths in Proteins by Nuclear Magnetic Resonance Methods." *Protein Struct. Funct. Genet.* **1999**, *35*, 275-282.

(41) Delorbe, J.E.; Clements, J.H.; Teresk, M.G.; Benfield, A.P.; Plake, H.R.; Millspaugh, L.E.; Martin, S.F. "Thermodynamic and Structural Effects of Conformational Constraints in Protein-Ligand Interactions. Entropic Paradoxy Associated With Ligand Preorganization." *J. Am. Chem. Soc.* **2009**, *131*, 16758-16770.

(42) Ettmayer, P.; Fance, D.; Gounarides, J.; Jarosinski, M.; Martin, M. S.; Rondeau, J. M.; Sabio, M.; Topiol, S.; Weidemann, B.; Zurini, M.; Bair, K. W. "Structural and Conformational Requirements for High-Affinity Binding to the SH2 Domain of Grb2." *J. Med. Chem.* **1999**, *42*, 971-980.

(43) Shi, Y.; Zhu, C.Z.; Martin, S.F.; Ren, P. "Probing the Effect of Conformational Constraint on Phosphorylated Ligand Binding to an SH2 Domain Using Polarizable Force Field Simulations." *J. Phys. Chem. B* **2011**, *133*, 18518-18521.

(44) Myslinski, J.M.; Clements, J.H.; Delorbe, J.E.; Martin, S.F. "Protein-Ligand Interactions: Thermodynamic Effects Associated with Increasing the Length of an Alkyl Chain." *ACS Med. Chem. Lett*, **2013**, *4*, 1048-1053.

(45) Bonaparte, A. C. "Synthesis of β-Heteroaryl Propionates via Trapping of Carbocations with π-Nucleophiles, Efforts Towards the Total Synthesis of Acutumine, and the Design, Synthesis, and Thermodynamics of Protein-Ligand Interactions at the Src SH2 Domain." Dissertation, The University of Texas at Austin, **2013**.

(46) Jimenez, J.M.; Rife, J.; Ortuño, R.M. "Enantioselective Total Syntheses of Cyclopropane Amino Acids: Natural Products and Protein Methanologs." *Tetrahedron: Asymmetry* **1996**, *7*, 537-558.

(47) Groth, U.; Halfbrodt, W.; Schöllkopf, U. "Asymmetric Synthesis of (+)-(1*R*,2*S*)-*allo*-Coronamic Acid." *Liebigs Annalen der Chemie* **1992**, *4*, 351-355.

(48) Schmidt, U.; Lieberknecht, A.; Wild, J. "Amino Acids and Peptides; XLIII. Dehydroamino Acids; XVIII. Synthesis of Dehydroamino Acids and Amino Acids from *N*-Acyl-2-(dialkyloxyphosphinyl)-glycin Esters; II." *Synthesis* **1981**, 53-60.

(49) Schmidt, U.; Lieberknecht, A. "Facile Preparation of *N*-Acyl-2-(diethoxyphosphoryl)glycine Esters and Their Use in the Synthesis of Dehydroamino Acid Esters." *Angew. Chem. Int. Ed. Engl.* **1982**, *21*, 776-777.

(50) Yamaguchi, K.; Une, F.; Tabata, S.; Kinoshita, M. "Synthesis of Glycerophosphonolipids Containing Aminoalkylphosphonic Acids." *J. Chem. Soc. Perkin Trans. 1* **1986**, 765-770.

(51) Schmid, C. R.; Bryant, J. D. "D-(*R*)-Glyceraldehyde Acetonide." *Org. Synth.* **1995**, *72*, 6-13

(52) Williams, R.M.; Aldous, D.J.; Aldous, S.C. "General Synthesis of β,γ-Alkynylglycine Derivatives." *J. Org. Chem.* **1990**, *55*, 4657-4663.

(53) Kelly, T.R.; Schmidt, T.E.; Haggerty, J.G. “A Convenient Preparation of Methyl and Ethyl Glyoxylate.” *Synthesis* **1972**, 542-545.

(54) Roche, S.P.; Samanta, S.S.; Gosselin, M.J. “Autocatalytic One Pot Orchestration for the Synthesis of α-Arylated, α-Amino Esters.” *Chem. Commun.* **2014**, *50*, 2632-2634.

(55) Schmidt, U.; Lieberknecht, A.; Kazmaier, U.; Griesser, H.; Jung, G.; Metzger, J. “Amino Acids and Peptides; 75. Synthesis of Di- and Trihydroxyamino Acids-Construction of Lipophilic Tripalitoyldihydroxy-α-amino Acids.” *Synthesis* **1991**, 49-55.

(56) Lebel, H.; Marcoux, J.-F.; Molinaro, C.; Charette, A. B. “Stereoselective Cyclopropanation Reactions.” *Chem. Rev.* **2003**, *103*, 977-1050.

(57) Charette, A.B.; Lebel, H. “Diastereoselective Cyclopropanation of Chiral Allylic Alcohols: A More Efficient Reagent for the Relative Stereocontrol.” *J. Org. Chem* **1995**, *60*, 2966-2967.

(58) Furukawa, J.; Kawabata, N.; Nishimura, J. “Synthesis of Cyclopropanes by the Reaction of Olefins with Dialkylzinc and Methylene Iodide.” *Tetrahedron* **1968**, *24*, 53-58.

(59) Denmark, S. E.; Edwards, J. P. “A Comparison of (Chloromethyl)- and (Iodomethyl)zinc Cyclopropanation Reagents.” *J. Org. Chem*. **1991**, *56*, 6974-6981.

(60) Yang, Z.; Lorenz, J. C.; Shi, Y. “Exploring New Reactive Species for Cyclopropanation.” *Tetrahedron Lett.* **1998**, *39*, 8621-8624.

(61) Charette, A. B.; Francoeur, S.; Martel, J.; Wilb, N. “New Family of Cyclopropanating Reagents: Synthesis, Reactivity, and Stability Studies of Iodomethylzinc Phenoxides.” *Angew. Chem. Int. Ed.* **2000**, *39*, 4539-4542.

(62) Morikawa, T.; Sasaki, H.; Mori, K.; Shiro, M.; Taguchi, T. "Simmons-Smith Reactions of Fluoroallyl Alcohol Derivatives." *Chem. Pharm. Bull.* **1992**, *40*, 3189-3193.

(63) Das, M.K.; Zuckerman, J.J. "Synthesis and Transformations of Phosphorus Imidazolines (1,3-diaza-2-phospholidines)." *Inorg. Chem.* **1971**, *10*, 1028-1030.

(64) Corey, E.J.; Hopkins, P.B. "A Mild Procedure for the Conversion of 1,2-diols to Olefins." *Tetrahedron. Lett.* **1982**, *23*, 1979-1982.

(65) Chen, J.; Corbin, S. P.; Holman, N. J. "An Improved Large Scale Synthesis of the Schöllkopf Chiral Auxiliaries: (2*R*)- and (2*S*)-2,5-Dihydro-3,6-dimethoxy-2-isopropylpyrazine." *Org. Proc. Res. Dev.* **2005**, *9*, 185-187.

(66) DeLorbe, J. E. "Design, Synthesis, and Evaluation of Conformationally-Constrained Grb2 SH2 Ligands and a Concise Total Synthesis of Lycopladine A." Dissertation, University of Texas at Austin, **2010**.

(67) Cramer, D. L. "Design, Synthesis, and Calorimetric Studies on Protein-Ligand Interactions: Apolar Surface Area, Conformational Constraints, and Application of the Topliss Decision Tree." Dissertation, University of Texas at Austin, **2013**.

(68) Brimble, M.A.; Harris, P.W.R.; Sieg, F. "Analogs of glycyl-prolyl-glutamate." Patent WO2006127702 A2.